







Article

The Utilization of a 3D Groundwater Flow and Transport Model for a Qualitative Investigation of Groundwater Salinization in the Ca Mau Peninsula (Mekong Delta, Vietnam)

Tran Viet Hoan ^{1,2,*} , Karl-Gerd Richter ³ , Felix Dörr ¹ , Jonas Bauer ^{1,*} , Nicolas Börsig ¹ , Anke Steinel ⁴ ,
Van Thi Mai Le ², Van Cam Pham ¹, Don Van Than ² and Stefan Norra ⁵

¹ Institute of Applied Geosciences, Karlsruhe Institute of Technology (KIT), Adenauerring 20b, 76131 Karlsruhe, Germany; nicolas.boersig@kit.edu (N.B.)

² National Center for Water Resources Planning and Investigation (NAWAPI), No. 93, lane 95, Vu Xuan Thieu Street, Sai Dong Ward, Long Bien District, Hanoi 100000, Vietnam

³ Aquantec Company for Water and Environment GmbH, Am Zwinger 5, 76227 Karlsruhe, Germany; richter@aquantec-gmbh.de

⁴ German Federal Institute for Geosciences and Natural Resources (BGR), Stilleweg 2, 30655 Hannover, Germany

⁵ Institute of Environmental Sciences and Geography, Soil Sciences and Geoecology, Campus Golm, Potsdam University, Building 12, 14476 Potsdam, Germany

* Correspondence: hoan.tran@kit.edu (T.V.H.); jonas.bauer@kit.edu (J.B.)

Abstract: The Ca Mau Peninsula (CMP), the southernmost region of the Mekong Delta, is increasingly threatened by groundwater salinization, posing severe risks to both the freshwater supply and land sustainability. This study develops a three-dimensional, density-dependent groundwater flow and salinity transport model to investigate salinization dynamics across the CMP's complex multi-aquifer system. Unlike previous studies that largely rely on model calibration, this research introduces a novel approach by systematically deriving the spatial distribution of longitudinal dispersivity based on sediment characteristics. Moreover, detailed land use mapping is integrated to assign spatially and temporally variable Total Dissolved Solids (TDS) values to the uppermost layers, thereby enhancing the model realism in areas where monitoring data are limited. The model was utilized not only to simulate the regional salinity evolution, but also to critically evaluate conceptual hypotheses related to the mechanisms driving groundwater salinization. Results reveal a strong influence of seasonal and land use factors on salinity variability in the upper aquifers, while deeper aquifers remain largely stable, affected primarily by paleosalinity and localized pumping. This integrated modeling approach contributes to a better understanding of regional-scale groundwater salinization and highlights both the potential and the limitations of numerical modeling under data-scarce conditions. The findings provide a valuable scientific basis for adaptive water resource management in vulnerable coastal zones.

Keywords: salinity modeling; groundwater transport modeling; hydrogeology; aquifers system; Vietnam; saltwater intrusion; Ca Mau Peninsula; Kien Giang; Bac Lieu



Academic Editor: Yong Xiao

Received: 25 March 2025

Revised: 10 May 2025

Accepted: 12 May 2025

Published: 20 May 2025

Citation: Hoan, T.V.; Richter, K.-G.; Dörr, F.; Bauer, J.; Börsig, N.; Steinel, A.; Le, V.T.M.; Pham, V.C.; Than, D.V.; Norra, S. The Utilization of a 3D Groundwater Flow and Transport Model for a Qualitative Investigation of Groundwater Salinization in the Ca Mau Peninsula (Mekong Delta, Vietnam). *Hydrology* **2025**, *12*, 126. <https://doi.org/10.3390/hydrology12050126>

Copyright: © 2025 by the authors. Licensee MDPI, Basel, Switzerland. This article is an open access article distributed under the terms and conditions of the Creative Commons Attribution (CC BY) license (<https://creativecommons.org/licenses/by/4.0/>).

1. Introduction

Groundwater salinization is increasingly recognized as a critical global issue, threatening freshwater resources essential for domestic, agricultural, and economic activities in coastal regions [1–4]. This phenomenon is exacerbated by multiple stressors, including

climate change, rising sea levels, and intensive groundwater extraction [5,6], highlighting the need for the improved understanding and management of coastal groundwater resources [7].

The Ca Mau Peninsula (CMP), located at the southernmost region of the Mekong Delta (MKD), is one of the regions most affected by groundwater salinization [8]. For local communities who rely heavily on groundwater, particularly during the dry season [9], excessive groundwater extraction has led to notable declines in groundwater levels (Figure 1). Additionally, upstream dam construction on the Mekong River significantly reduces freshwater inflow, intensifying dry season saltwater intrusion inland [10,11]. However, saltwater intrusion pathways remain inadequately understood due to geological complexity and data limitations, necessitating detailed hydrogeological modeling.

The hydrogeological structure of the CMP comprises seven aquifers and seven aquitards [12,13]. While aquitards were traditionally viewed as continuous barriers, recent studies highlight significant heterogeneity and interconnectedness among aquifers [6,14]. Observations show synchronized dynamics of the groundwater levels across multiple aquifers, suggesting either hydraulic connectivity or loading effects from external stresses [15].

To underscore the urgency of the situation, Figure 1 illustrates the decline in groundwater levels across various aquifers in the CMP, providing direct visual context for the modeling objectives that follow.

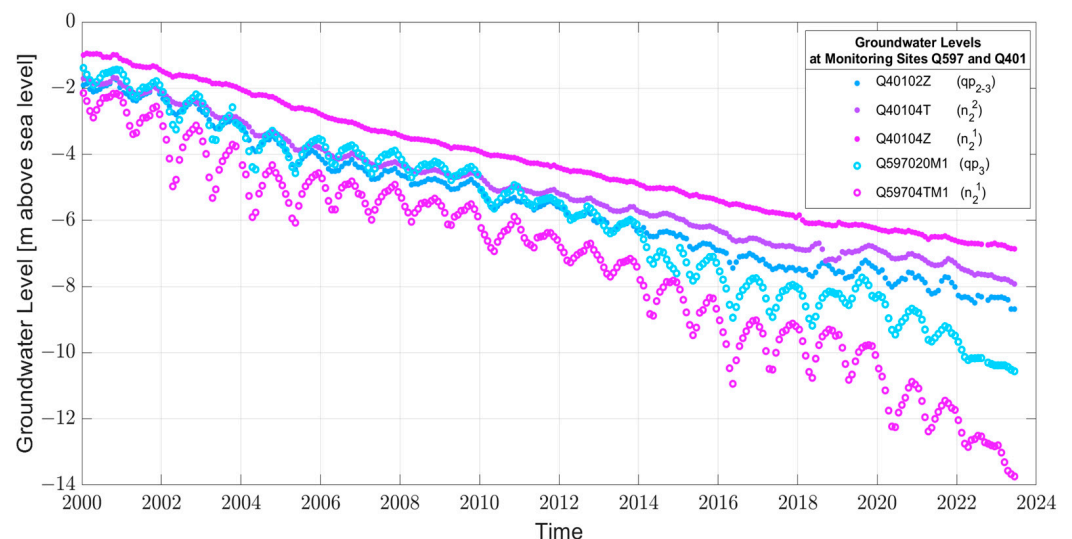


Figure 1. Monthly averaged groundwater levels in monitoring well groups, Q597 and Q401, located in the Ca Mau Peninsula; for the location see Figure 2, and for different aquifers (upper Pleistocene—qp₃; Upper–Middle Pleistocene—qp₂₋₃; Middle Pliocene—n₂²; Lower Pliocene—n₂¹) see Figure 3 (source of data: the NAWAPI).

Over the past decades, groundwater flow and salinization models have been developed for Vietnam [16–18], as well as for the MKD in particular [13,19,20]. Modeling approaches have primarily employed the MODFLOW software [21] and have mostly covered large areas. However, a recent development includes a local high-resolution groundwater model specifically designed for the CMP by [12].

Due to the limited availability of spatially distributed, continuous salinity measurement data, we propose a salinity transport model based on the hydrogeological model of [12] to assess potential salinity pathways.

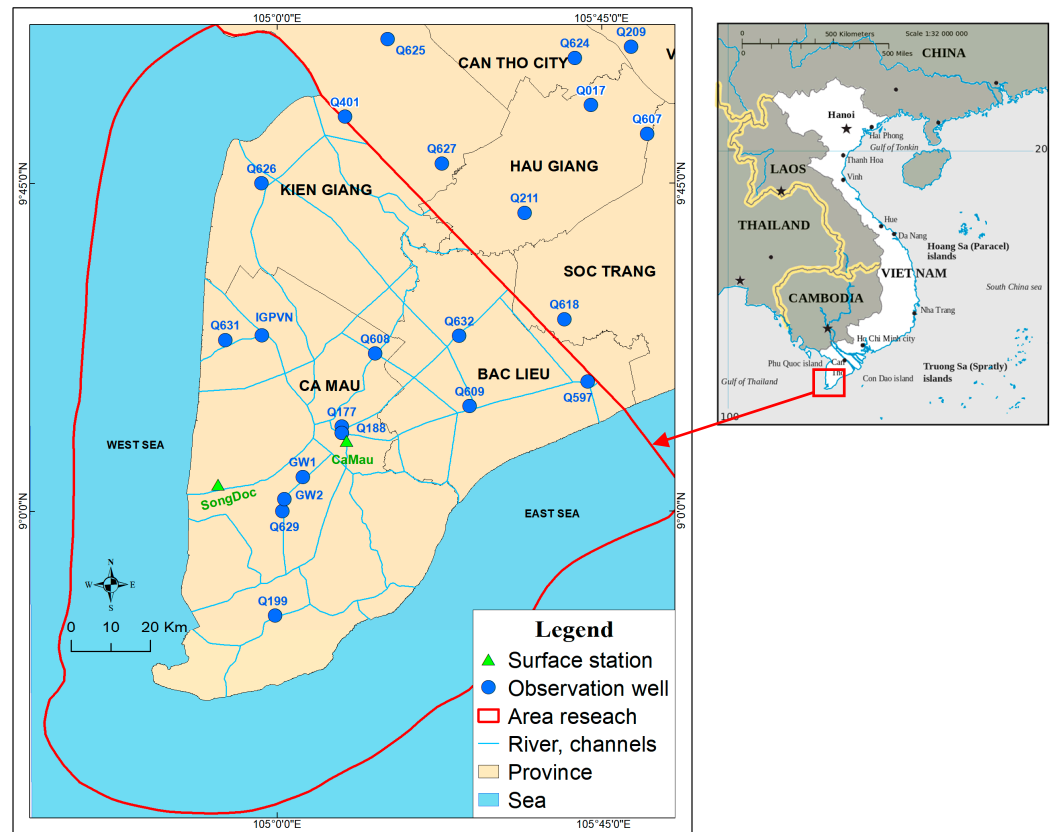


Figure 2. The location of the study area on the Ca Mau Peninsula showing the extent of the model area and observation wells (sources of data: NAWAPI, Esri, HERE, Garmin, © OpenStreetMap contributors, and the GIS user community).

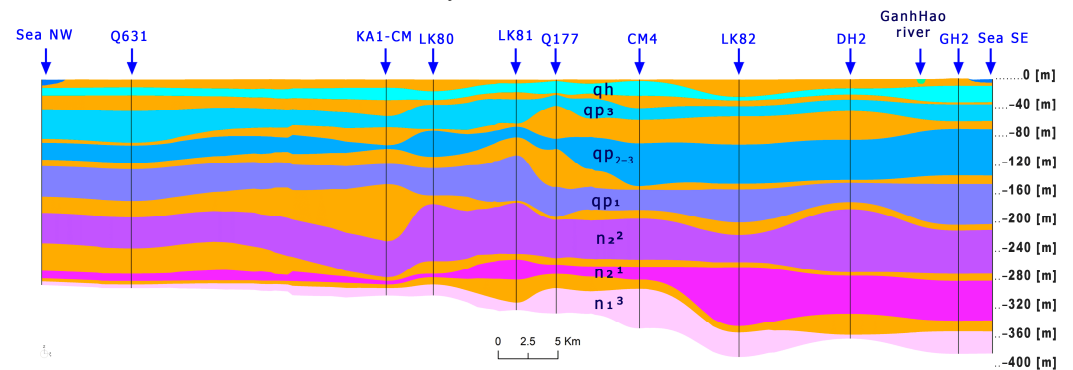


Figure 3. The hydrogeological structure of the Ca Mau Peninsula. Aquitards are shown in orange, and aquifers range in color from blue to magenta (modified after [12]).

Based on the data analysis and the knowledge from the hydrogeological model, we formulate and evaluate the following hypotheses based on observed salinity trends and hydrogeological modeling:

- (a) “There is no lateral saline intrusion from the ocean into the deeper aquifer”.

This hypothesis suggests no horizontal saltwater movement into the deeper aquifer, depending on the geological and hydrological conditions such as the extent and continuity of the aquitards.

- (b) “Different land use classes impact the salinity in the qh aquifer and contribute to the high spatial variability of the salinity in the qh aquifer”.

This hypothesis indicates spatial salinity variability driven by land use impacts on infiltration, runoff, and recharge processes.

- (c) “Interannual variations in the surface water salinity in the river and channel system, as well as in mangrove, rice, and shrimp farming areas, could cause the high variability in the salinity in the qh aquifer”.

This hypothesis emphasizes climatic, precipitation, and anthropogenic influences on salinity dynamics in shallow aquifers.

- (d) “Salinity variations in the deeper aquifers might be caused by the extraction of water during pumping”.

Based on recent field surveys conducted by the ViWaT research program [9,22] and data collected in Ca Mau Province, there has been a noticeable rise in the groundwater salinity levels over the past decade. This has led farmers and water suppliers to drill deeper wells to access freshwater, as previously utilized sources no longer meet quality standards (personal interviews with local farmers, 2022). However, monitoring data from the Vietnamese national groundwater network show no significant increase in salinity within the deeper aquifers [23]. This discrepancy suggests a need for further investigation to identify whether local factors, such as over-extraction or well-drilling practices, could be causing localized increases in salinity.

This study advances the understanding of saltwater intrusion by systematically deriving the spatial distribution of longitudinal dispersivity instead of relying solely on calibration, as commonly practiced in previous groundwater salinity models. Rather than focusing solely on optimizing the fit to available salinity measurements, our approach prioritizes improving the physical understanding of salinity transport processes through a hypothesis-driven methodology. While many studies traditionally adjust porosity to refine model performance, we highlight the critical role of dispersivity in controlling salinity patterns. A particularly notable contribution is the application of detailed land use maps to assign variable TDS values for the uppermost aquifer layer, where direct monitoring data are limited or unavailable. This method significantly enhances the spatial resolution and accuracy of groundwater salinity characterization at regional scales, providing an efficient and cost-effective alternative to traditional field-based measurements and interpolation techniques. The findings offer valuable insights into interactions between aquifer heterogeneity, dispersivity, and land use-driven salinity variations, establishing a refined methodology highly applicable for regional groundwater salinity assessments.

The primary objectives of this study are as follows: (1) to systematically derive the spatial distribution of longitudinal dispersivity; (2) to integrate detailed land use mapping to assign realistic TDS values in shallow aquifers; (3) to elucidate the dynamics and underlying mechanisms of groundwater salinization within a complex multi-aquifer system at the regional scale; and (4) to assess the practical limitations of applying the modeling approach.

2. Study Area

The study area aligns with that employed in our previous study [12]. It is located in the southernmost region of the MKD, Vietnam, covering the provinces of Ca Mau, Bac Lieu, and the lower part of Kien Giang (see Figure 2). The study area is located in a region strongly affected by climate change [24]. The region faces major challenges, described by [9] as the “loss of land and freshwater”, which includes processes such as coastal erosion, land subsidence, and the salinization of the surface and groundwater bodies.

Geologically, there have been multiple transgression and regression periods, resulting in several-hundred-meter-thick sequences of marine and fluvial sediment deposits [14]. In recent geological history, the area was created as a consequence of the uplift of the Himalayan Mountains and the associated erosion. This eroded material was transported by

the Mekong River and deposited in its delta, forming the CMP. These deposits also exhibit a certain degree of salinity from former transgression/regression processes.

With an average elevation of approximately 0.8 m [25] above sea level, the CMP lies at a relatively low altitude. The coastline of the model area is approximately 396 km long. The maximum ocean depth within a range of 30 km beyond the coastline is approximately 80 m. The salinity of the ocean water is 35 g/L on average [13,26]. The channel and river system of the CMP is strongly influenced by the ocean tides. Tidal amplitudes in the western sea reach a maximum of approximately 1 m, whereas in the eastern sea, amplitudes can reach up to 4 m [27]. This causes saline inflow into the channel and river system, with a maximum salinity of nearly 33 g/L in the river system [28]. The river system can be locally connected to the qh aquifer, as described by [29]. However, the surface water–groundwater interaction is considered to be limited in most areas, with the top aquitard being several meters thick [12], Figure 3 (cross-section).

The surface water network comprises a dense system of interlinked channels used for transportation and agricultural and aquacultural activities. However, the hydraulic interaction between the surface water network and the aquifer system does not extend down to qp_{2–3} [30]. The conceptual model of the groundwater system of the CMP consists of seven aquifers (from top to bottom: Holocene—qh; Upper Pleistocene—qp₃; Upper—Middle Pleistocene—qp_{2–3}; Lower Pleistocene—qp₁; Middle Pliocene—n₂²; Lower Pliocene—n₂¹; and Upper Miocene—n₁³; Figure 3). These aquifers are separated from each other by aquitards. However, the continuity of these aquitards has not yet been fully clarified and is therefore examined in this evaluation.

The groundwater in the deep aquifers in the MKD region consists of brackish, saline, and fresh types. In previous studies, the determination of the groundwater age was inconclusive, ranging from recent to older than 45 ka, but with an increasing trend from the Pleistocene to Miocene aquifers [26,30]. The saline water in the deep aquifers could result from the diffusion of saline pore water and/or past/present salt intrusion into the freshwater resources. The interaction between the deeper aquifers might be caused by the natural conditions (e.g., locally thin aquitard layer, hydrogeological windows, and hydraulic gradients) or anthropogenic factors (e.g., number of production wells, leakage along the well structure, and underground construction) [9].

This study focuses on qp_{2–3} and n₂² aquifers, as these are the most exploited aquifers in the model area, as mentioned in [12]. The qp_{2–3} and n₂² accounted for 63.7% (361,580 m³/day in 2019) and 29.7% (168,600 m³/day in 2019) of the total pumping in 2011. According to a survey conducted in 2019, residents in Ca Mau mainly use groundwater for diverse domestic purposes. However, only 25.4% of the respondents in the survey used groundwater from local household wells for drinking purposes [22]. The higher salinity in the qp_{2–3} aquifer is one reason for the minor use of its groundwater for drinking. In addition, high concentrations of other parameters (e.g., Fe, Mg, etc.) have been reported [4], leading to a reduced use of water from qp_{2–3} for drinking. Therefore, this study emphasizes the importance of qp_{2–3} and n₂².

Due to the presence of a thick clay layer at the top, the recharge to deeper aquifers in the study area is severely restricted. Consequently, groundwater in deeper aquifers primarily comprises paleowater, accumulated tens of thousands of years ago during historical transgression and regression periods. Over thousands of years, variations in transgression and regression have shaped the current salinity patterns in deep aquifers, leading to complex interactions between ancient saline water and present groundwater dynamics. This characteristic strongly influences the groundwater salinity distribution and dynamics within the system.

3. Data Collection

Despite these modeling advancements, the available data for the evaluation of ground-water salinity in the CMP remain limited. Groundwater salinity data in the CMP have been collected primarily through two distinct approaches:

- Sampling campaigns at various observation wells in different aquifers, with the laboratory analysis of Total Dissolved Solids (TDS) since 2011 with two measurements per year (dry and rainy season);
- Electrical Conductivity (EC) measurements (data logging sensor) with a calibration factor for TDS calculations, implemented since 2019, at various observation wells in different aquifers.

To ensure comprehensive data coverage, salinity data were collected from multiple sources, including the national groundwater monitoring network [31] and international research cooperation projects, such as the ViWaT project (<https://www.viwat.info/english/21.php> (accessed 20 August 2023)) and the IGPVN (<https://igpvn.vn/> (accessed 20 August 2023)) project from 2013 to 2022, which cover key study areas, including Ca Mau, Kien Giang, Soc Trang, and Bac Lieu.

For salinity measurements, two distinct methodologies were employed in the study area. The first approach entailed the laboratory analysis of water samples utilizing standard procedures. While some samples were collected biannually during both the dry and rainy seasons [32], others were based on one-time sampling. In contrast, the second method involved continuous measurements using Electrical Conductivity.

It should be noted that EC and TDS values obtained over long-term monitoring periods can exhibit certain inaccuracies due to various factors, including the prolonged observation of well operations, sampling technique, pumping duration, and analytical procedures [33,34]. These factors inherently increase uncertainty in EC and TDS measurements. Nevertheless, this variability reflects the natural complexity and inherent uncertainty of real groundwater systems, particularly in shallow aquifers (qh). Therefore, these discrepancies are considered an inevitable component in the analysis and evaluation of modeling results.

These salinity measurements are crucial for assessing seawater intrusion in coastal areas. The assessment of seawater intrusion into the groundwater in the coastal areas of Vietnam relies predominantly on the TDS and EC measurements. However, our data collection process revealed the existence of numerous conversion factors between the EC and TDS across different studies, which creates a larger uncertainty in the data.

To address this uncertainty and improve the spatial resolution of the salinity data, various interpolation methods can be employed. Saline and freshwater areas can be distinguished using the interpolation method in space for point measurements. Alternatively, regionalizing methods can be used, as presented by [35]. The dataset, available on a 1 km by 1 km grid, incorporated groundwater points with TDS and wells with geophysical logging via indicator kriging. An additional dataset for Ca Mau Province is from [23]. To regionalize these data for each aquifer, a detailed data analysis and interpolation using the “Ordinary kriging [36] in the ArcGIS geostatistical analyst toolbox, as the best linear unbiased estimator” [23] was carried out. The result was a homogenized dataset of salinity distributions for each aquifer. Therefore, in principle, two homogenized datasets are available for the CMP.

The time series of the measured data from 2011 to 2021 did not reveal any significant trend in the lower aquifers regarding salinization [23]. In Figure 4a, the measured TDS data for aquifer qh are presented, illustrating the entire period of observation from 2011 to 2024. While the assessment focuses on the 2011–2021 period, some monitoring wells in aquifer qh, such as Q177 and Q632, exhibited fluctuations in TDS concentrations over time; however, no clear increasing or decreasing trend was evident, particularly for well Q401

(Figure 4a). Overall, the available data do not suggest a long-term increase in salinity in aquifer qh on a regional scale.

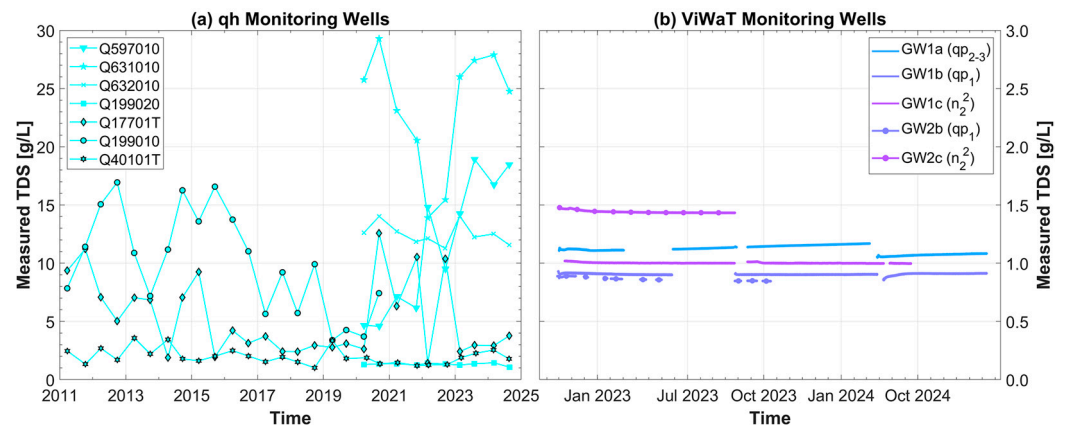


Figure 4. Examples of TDS time series of groundwater monitoring wells from (a) the NAWAPI (aquifer qh; period 2011–2024) and (b) the ViWaT project (well groups installed in 2022).

In Figure 4b, the automated EC monitoring data (converted to TDS) of groundwater wells in the ViWaT projects at two monitoring locations, GW1 and GW2, are visualized. The data showed that different levels of TDS were established at two sites in different aquifers over time. However, the observed change in the TDS in the aquifers was not significant.

4. Methodology

4.1. Approach to Salinity Transport Modeling

An adapted method for the assessment of saline intrusion was employed, based on numeric modeling but deviating from the conventional approach of calibrating the parameters for a transport model, due to the limited data availability (Figure 5). The method involves developing a simple model to calculate the longitudinal dispersion coefficient using a global dataset and verifying it with regionally developed coefficients, which were derived from the data collected in the study area. The main goal of our approach was to improve the understanding of the physical processes involved, rather than achieving the best fit for the few available salinity measurements.

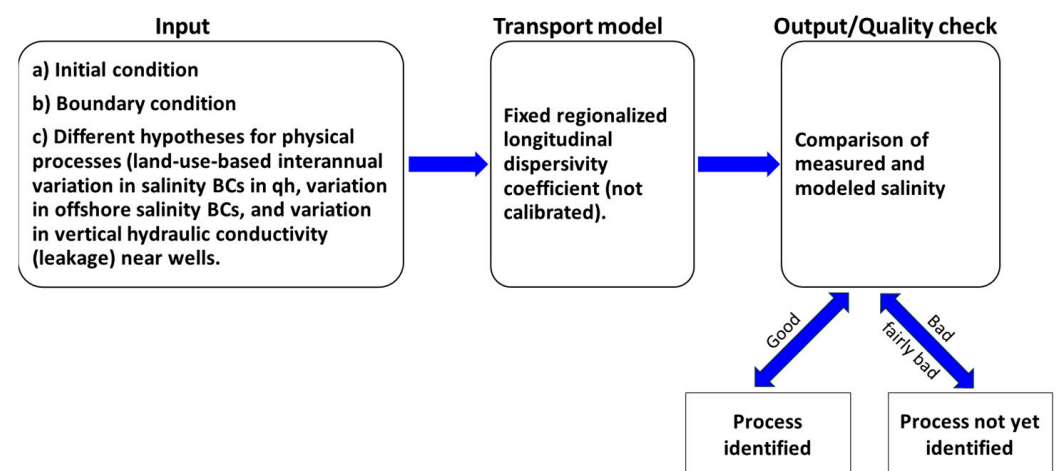


Figure 5. Conceptual framework for evaluating longitudinal dispersion coefficients in saltwater intrusion processes in the Ca Mau Peninsula. *Note: The four processes outlined in the model include additional mechanisms that may not fully correspond to the initial hypotheses but are considered relevant based on field observations.*

Our aim was to assess the significance of these hypotheses and glean insights into the dynamic processes governing groundwater salinization through the examination of various hypotheses against both measured and calculated salinity data. This approach emphasizes a more exploratory and hypothesis-driven analysis of salinity transport, allowing for the identification of important processes. Such an approach is promising and potentially insightful, particularly in situations with limited available salinity data.

Figure 5 illustrates the conceptual framework we used for evaluating salinity transport in the study area. While the initial hypotheses provided a foundational framework for evaluating salinity transport processes, the model incorporates additional mechanisms based on the field data and observed variability in the study area. These mechanisms, including the mixing and dispersion along the flow path and leakage through hydraulic windows, are considered essential for a comprehensive analysis of potential salinization pathways. The conceptual framework also accounts for the historical context of the groundwater system. Given the predominance of paleowater in deeper aquifers, initial salinity conditions in the groundwater model reflect historical salinity patterns resulting from past marine transgression and regression events. This assumption aligns with the field evidence showing distinct salinity interfaces and mixing patterns, as detailed in the Section 4.2.2, which are critical for understanding current salinity dynamics driven by hydraulic gradients from intensive groundwater extraction.

The output of the transient transport model is the concentration at each node in the model domain during the considered time period. The calculated concentration values can be compared to observed concentrations as well as to qualitative information (e.g., reports showing increasing salinity in some production wells). Our approach highlights the iterative nature of model development and refinement. If the simulation results show a good agreement between the measured and calculated salinity in terms of the trend and the order of magnitude, it suggests that the identified processes and the model parameters used could represent real-world conditions. This alignment provides confidence in our model's ability to predict salinity transport within the study area. The spatial discretization of the model was designed to support large-scale and long-term salinity simulations. A spatially variable mesh with local refinement was applied in sensitive areas; the details of the mesh configuration are provided in Section 4.2.1.

In contrast, if the simulation results do not match the measured salinity well, it signals the need for further investigation. This may involve the identification of additional or alternative physical processes that impact salinity transport but were not adequately considered in the initial model. It could also prompt a re-evaluation of the chosen model parameters and assumptions.

The goal of this study was to continuously refine and improve the model by incorporating new insights, data, and adjustments to better capture the complexities of the salinity transport system. This iterative process is common in scientific modeling, where the feedback loop between model predictions and real-world observations helps enhance the accuracy and reliability of the model over time.

4.2. Saline Intrusion Model Setup

Figure 6a illustrates the process of enhancing the existing flow model [12], transforming it into a variable-density transient transport model with a subsequent sensitivity analysis. Figure 6b provides a three-dimensional conceptual representation of the aquifer–aquitard system used in the model, helping visualize the spatial structure and layering relevant to salinity transport.

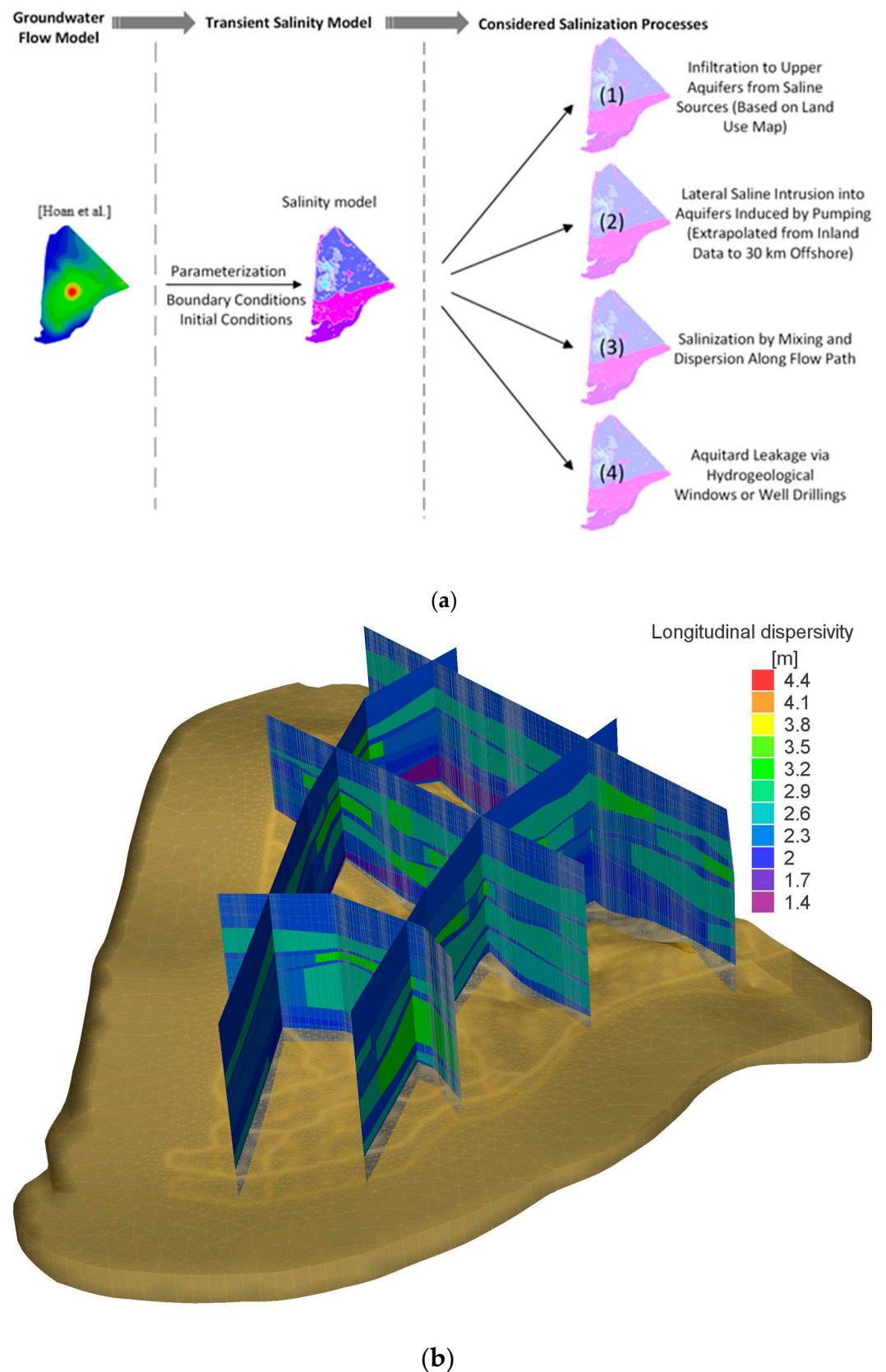


Figure 6. (a) The flowchart of the integrated groundwater flow [12] and salinity modeling approach for evaluating potential saltwater intrusion processes in the MKD. (b) A three-dimensional schematic representation of the hydrogeological model, showing the spatial layering of aquifers and aquitards with corresponding longitudinal dispersivity values assigned to each sediment type.

The density-dependent transient transport model for the CMP was set up with the software FEFLOW [37] for the time period from 2011 to 2024. The following salinization processes in the CMP were considered in the model:

1. Infiltration from saline surface water sources (rivers, canals, aquaculture ponds, salt production, and tidal inundations) into the upper aquifers as identified by the land use map;
2. Lateral saline intrusion from the offshore areas into the aquifer system induced by pumping, assuming that freshwater/saline water in deep aquifers is extrapolated from inland data up to 30 km offshore;
3. Salinization by mixing and dispersion from areas with higher salinity to areas with lower salinity along the flow path;
4. Downward or upward leakage from one aquifer to another through hydraulic windows in the aquitard, either naturally or from drilled wells. Although not included in the current model, this process is considered relevant to understanding salinity changes in the region.

4.2.1. Groundwater Flow Model

The groundwater flow model used as the basis for the salinity transport simulation was originally developed for the CMP by [12]. The original model covers a total area of approximately 19,900 km², including Ca Mau Province and parts of adjacent provinces, with approximately 9600 km² representing the land area. It was constructed using the finite-element software FEFLOW with a triangular finite-element mesh, featuring a spatially variable resolution. The mesh was refined to element sizes of 2–10 m near monitoring wells, extraction wells, rivers, and channels. Elsewhere, element sizes were gradually increased up to 2.5 km. Vertically, the model is structured into seven aquifers and seven interbedded aquitards. The boundary conditions of the flow model consist of a Dirichlet boundary condition (hydraulic head BC) at the northern boundary based on observed groundwater levels, no-flow boundary conditions along offshore boundaries, and Cauchy-type boundary conditions representing surface water–groundwater interactions in rivers and channels. The groundwater recharge was applied at a rate of approximately 1% of the monthly average precipitation. The flow model was simulated as a transient model from January 2011 to December 2020, using monthly time increments.

The understanding of the salinization process in the CMP is important for the model. Salinization in the upper aquifers (q_h , q_{p3}) is influenced by the intrusion from the river and channel system above and from the interaction between the sea and land beneath the ground surface. Additionally, we assume an influence from shrimp and rice farming practices, salt production, and groundwater abstraction. We also assume the presence of freshwater below the sea floor. These processes are simulated with the model setup.

4.2.2. Mass Transport Model

For the mass transport model, the TDS was used to represent salinity, as it is a widely accepted proxy in groundwater studies, particularly in coastal aquifers where detailed ionic composition data may be limited. This approach follows previous studies [13,26,35], which have demonstrated that the TDS provides a reliable spatial representation of salinity. During the model validation period, the observed TDS values from a total of 14 well groups were used for the period of 2011–2024. The transient transport model was run using monthly time steps to capture seasonal and interannual variations throughout the simulation period. For model comparison and analysis, observed TDS data were incorporated twice per year (representing the dry and rainy seasons) at each monitoring location. This approach enabled the model to effectively reflect seasonal salinity dynamics, particularly strongly

expressed in the shallow aquifer (qh), while also capturing long-term salinization trends observed in deeper aquifers (qp₃, qp₂₋₃, qp₁, n₂², and n₂¹).

Model Boundary Conditions

The following boundary conditions (BCs) were considered:

- (1) Seawater intrusion was implemented as Dirichlet BCs with defined concentrations. For Layer 1–Layer 5, representing aquifers qh and qp₃, this was set to 35 g/L (similar to the current TDS of seawater), while for Layer 6–Layer 14, which represent the main exploited aquifers (freshwater to slightly brackish water), this was set to 3 g/L [38] at the model boundary offshore.
- (2) No boundary conditions for salinity were defined at the northern model boundary. As there is a flow boundary condition defined at the northern model boundary, the FEFLOW software automatically generates a salinity boundary condition to adapt the concentration of the inflowing water to maintain the concentration near the boundary.
- (3) The land use-based estimation of human activities influencing the salinity in the qh aquifer was determined using land use maps [39] (Figure 7, left side). For most land use classifications, a constant salinity concentration BC was used (see Figure 7, right side) for the top layer and the qh aquifer depending on the predominant land use class in each region. At selected locations, these boundary conditions were refined to time-varying fixed-concentration BCs according to the interannual dynamics illustrated in Figure 8 with monthly data.
- (4) Surface water–groundwater interaction: The channel and river system in the CMP is strongly influenced by the tidal system of the ocean as well as seasonal (dry/rainy) interactions. The water levels in the river and channel system were interpolated from measurements based on the mean monthly change in the water level. In addition, we used the measured mean monthly salinity data (Ca Mau and Song Doc stations) to interpolate the interannual variation in the surface water bodies, mangrove, and semi-intensive shrimp and salt production zones and implemented them as time-varying fixed-concentration BCs (shown in Figure 8).

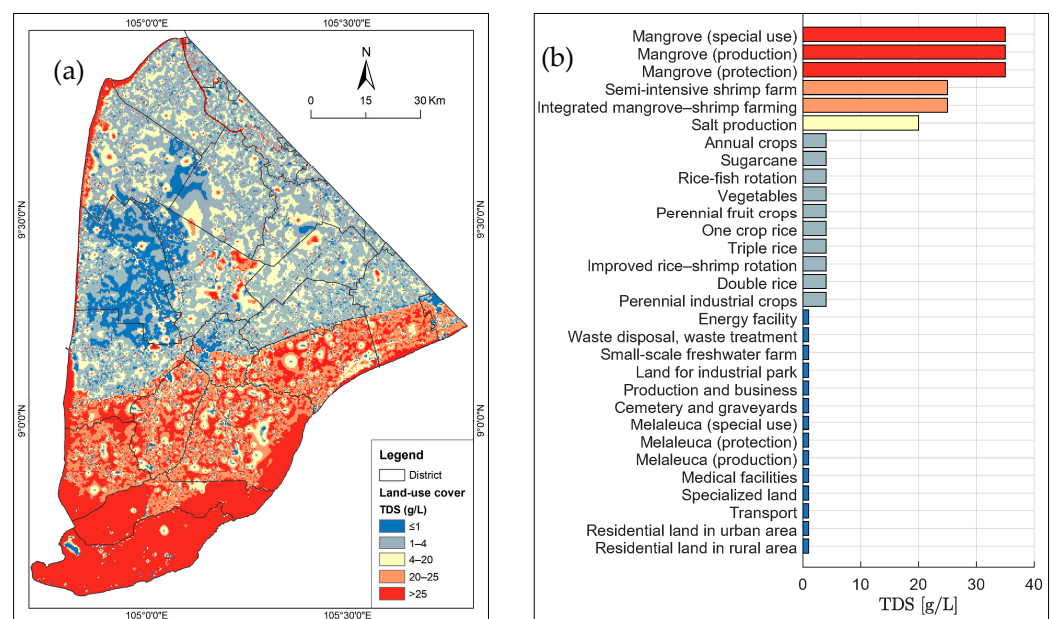


Figure 7. Land use-dependent salinity initialization (a) based on [39] and TDS classification based on land use (b).

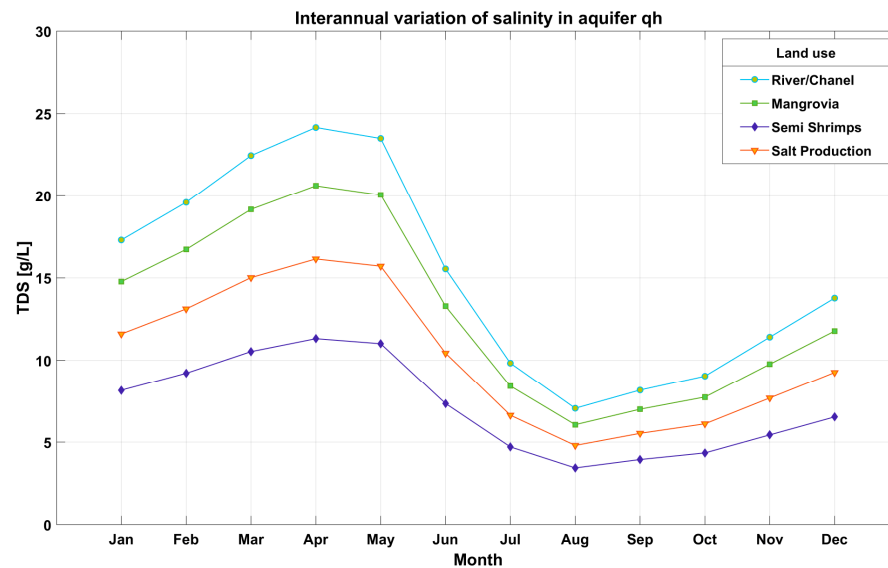


Figure 8. Mean monthly salinity for different land use types applied for model boundary conditions in aquifer qh and the top layer (derived from the salinity of surface water monitoring stations of Song Doc and Ca Mau, period 2012–2020).

Initial Conditions

At the beginning of the simulation (January 2011), the initial TDS concentration had to be defined for every node in the model. The initial conditions were determined based on the limited information available, specifically the salinity data collected simultaneously across different locations. All the salinity data available in different locations were utilized to establish the initial horizontal salinity values.

A combined dataset was established from the regionalized data of the IGPVN project [23] for the aquifers qp₃, qp₂₋₃, qp₁, n₂², and n₂¹ inside Ca Mau Province and interpolated values outside of Ca Mau Province based on the values measured during our data collection.

One of the challenges was determining the initial TDS concentration for the upper layers. There are many lakes, ponds, and rivers/channels, covering approximately 60% of the study area. However, their common feature is that the salinity varies seasonally. Data on these changing salinity levels are not available.

Therefore, the salinity in Layer 1 and Layer 2 (qh) was determined according to the zoning of the land use types, combined with survey data from some specific point groups. For the upper aquitards, the same initial conditions as in the upper aquifer were applied. For areas controlled by sluice gates, salinity measurements vary within a relatively small range. Consequently, the TDS value is considered to be a boundary condition that is constant over time for areas controlled by sluice gates. As for the remaining regions and land use types, their salinity variations were estimated through interpolation based on seasonal changes throughout the year (as depicted in Figure 8). The initial conditions for the aquifers are illustrated in Figure 9.

Dispersivity Parameter Adaptation

Flow velocities and hydrodynamic dispersion coefficients are key parameters for the description of fluid and solute transport in porous media. The topic of dispersivity has been of great interest in the scientific community, particularly among those studying hydrology and contaminants and flow through porous media (e.g., [40–43]). Hydrodynamic dispersion includes both mechanical (advective) dispersion and molecular diffusion. For low fluid velocities, solute dispersion is dominated by molecular diffusion; for high velocities,

advection becomes dominant, but the contribution of diffusion cannot be neglected. In this study, we did not calibrate the longitudinal dispersion coefficient but instead derived the spatial distribution of the longitudinal dispersion coefficient.

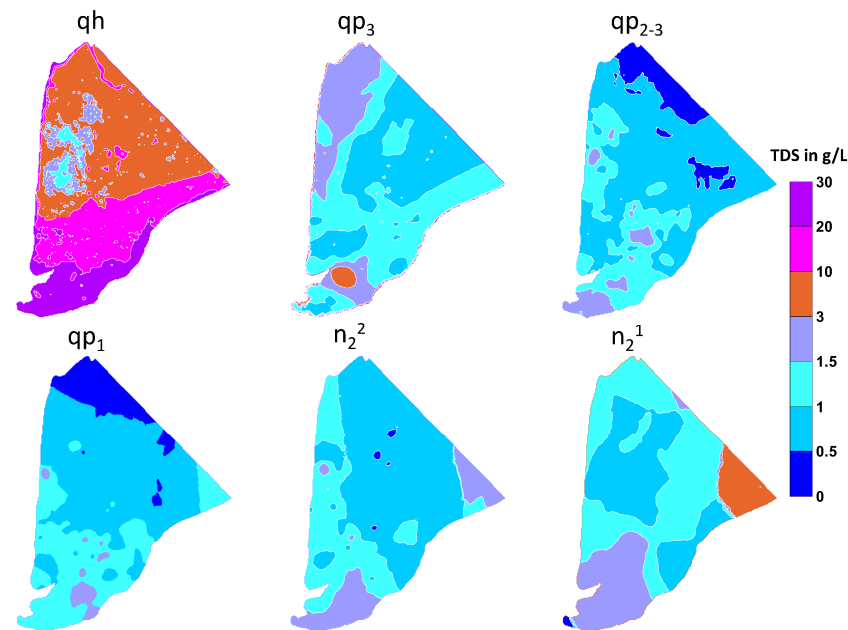


Figure 9. The spatial distribution of the initial salinity (January 2011) for the aquifers qh, qp3, qp2-3, qp1, n_2^2 , and n_2^1 .

The following dependencies of the longitudinal dispersion on the soil and sediment are known from the literature:

1. The longitudinal dispersivity coefficients for homogeneous soil and layered heterogeneous sediments show that stratification affects the longitudinal dispersivity coefficient, and the longitudinal dispersivity coefficients for layered heterogeneous sediments are nearly half than those in homogeneous sediments [44–47].
2. The longitudinal dispersion coefficient is influenced by the distance of travel, and its values undergo changes as the distance increases. In both homogeneous and layered heterogeneous sediments, the dispersion coefficient's values increase by a factor of 2.5 with the expansion of the horizontal travel distance [47–49].
3. There is also a dependency of the longitudinal dispersivity coefficient on the sediment type. From sand to clay, the longitudinal dispersion coefficient decreases with the smaller grain size of the material.

We set up a simple regionalized model for the calculation of the longitudinal dispersion coefficient in terms of average parameters from the Waterloo Hydrologic Enviro-Base, modified by the mentioned dependencies 1 and 2. We verified this regionalized longitudinal dispersion coefficient with local literature values [50].

Therefore, in this study, the Waterloo Hydrogeologic Enviro-Base [50] was used to calculate the average longitudinal dispersivity coefficients and average flow distances for different sediment types in the multilayered aquifer system of the CMP.

These averaged longitudinal coefficients were normalized (i.e., normalized dispersion coefficient) by dividing by the averaged flow distance (Figure 10a). The dependency of the normalized dispersion coefficient was fitted by the regression shown in Figure 10a. To recalculate the longitudinal dispersion coefficient for every soil type, an estimated flow distance of about 50 m was selected.

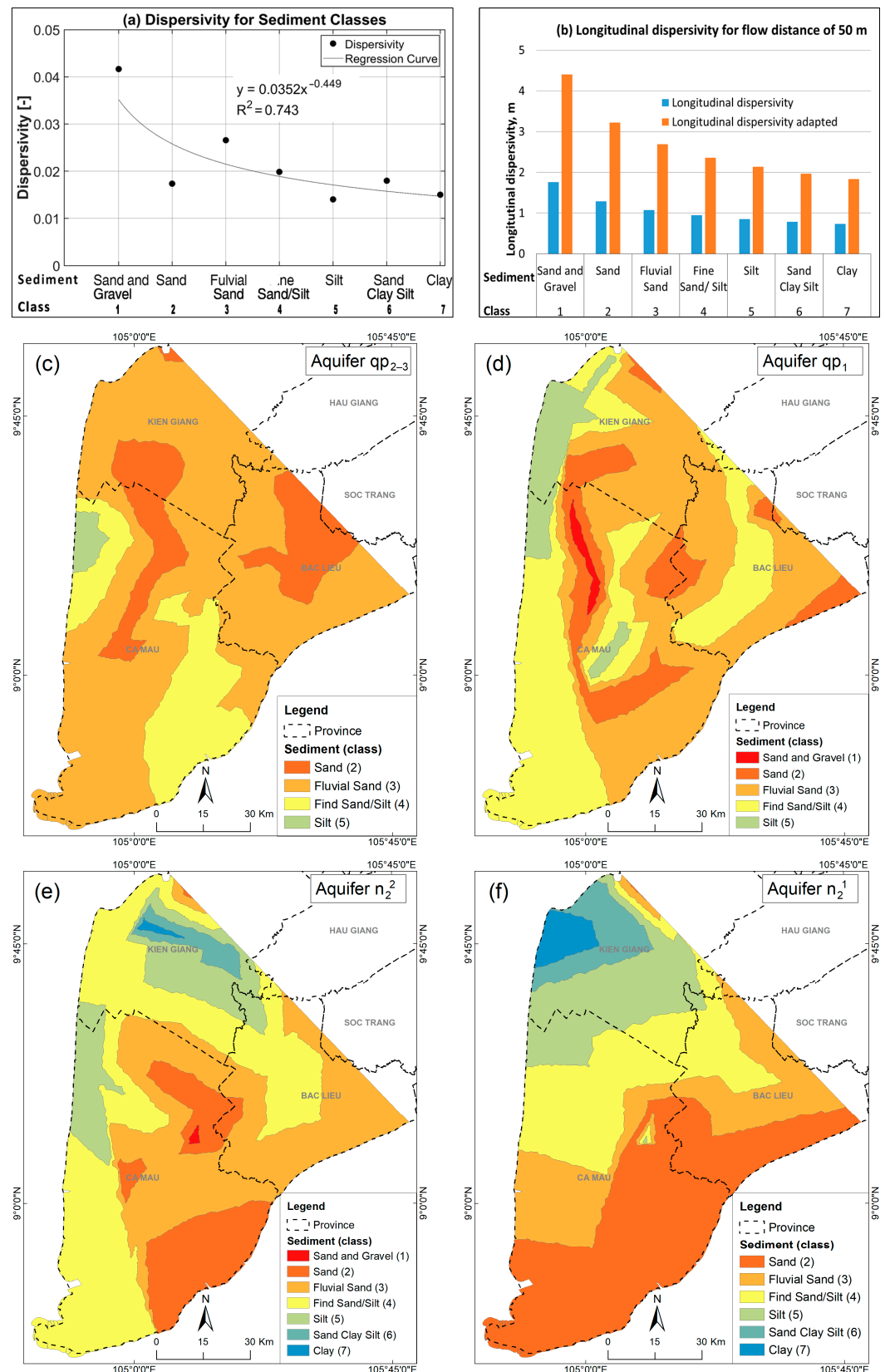


Figure 10. (a) The dependency of longitudinal dispersivity on the sediment class as demonstrated by [26], based on flow meter data; (b) longitudinal dispersivity coefficient (m) for different sediment classes based on a flow distance of 50 m for different sediment classes; and (c–f) sediment classes for different aquifers, qp₂₋₃, qp₁, n₂², and n₂¹ [51], used for the regionalization of the longitudinal dispersivity coefficient.

According to point one, we assumed that the sediments were homogeneous within the sediment classes presented in Figure 10, because detailed information about the sediment structure was not available. Thus, the longitudinal dispersivity was multiplied by a factor of 2.5 and by a 50 m flow distance. The regional distributions for the sediment type-based coefficients for aquifers qp_{2-3} , qp_1 , n_2^2 , and n_2^1 are shown in Figure 10c–f.

To validate the derived longitudinal dispersivity coefficients for the study area, they were compared to those in the previous literature. Ref. [52] described a groundwater fieldwork pumping and tracer injection test in the Nghiem Xuyen commune, Thuong Tin district, Hanoi, where a salinized and fresh groundwater boundary exists in the Pleistocene aquifer. The tracer experiment was conducted during a 60 h pumping test. The result was a longitudinal dispersivity value of 2.5 m, with an effective porosity of 0.32. In four other reports [53–56] (Table 1), the longitudinal dispersivity was estimated from 20-day-long tracer tests using 150 kg of salt. The salt was injected during pumping tests after the water level reached a steady state (after 48–72 h). These longitudinal dispersivity coefficient results differ significantly due to many influencing factors, such as the pump rate throughout the pumping test, the pumping well not being cleaned before the experiment, the salt injection process, and asynchronous machinery. In addition, there are natural factors such as the heterogeneous nature of the sediment types.

Table 1. Overview of dispersivity coefficients from different reports in Vietnam.

Well Name	Aquifer	Longitudinal Dispersivity	Effective Porosity	Specific Storage	Average Filtration Velocity	Flow Distance	Location
		α_L (m)	n_e (%)	μ (m^{-1})	V (m/min)	m	
CM2E ⁽¹⁾	n_2^2	1.14	14.0	7.53×10^{-4}	4.54×10^{-2}		Ca Mau
BL4D ⁽²⁾	n_2^2	0.02	16.0	4.58×10^{-3}	4.20×10^{-3}	8.0	Bac Lieu
BL2B ⁽³⁾	qp_{2-3}	0.12	19.4	5.58×10^{-4}	8.90×10^{-4}	8.0	Bac Lieu
IGPVN 1.4 ⁽⁴⁾	n_2^2	0.09–1.1	11.5–29.50		$4.0\text{--}9.9 \times 10^{-5}$	10.09	Ca Mau
CHN5 ⁽⁵⁾	qp_1	2.5	32.00				Hanoi

Note: ⁽¹⁾ [56], ⁽²⁾ [54], ⁽³⁾ [53], ⁽⁴⁾ [57], and ⁽⁵⁾ [52].

The longitudinal dispersivity coefficient varied between 0.02 m and 2.5 m, with an effective porosity between 11.5% and 32%. Thus, the aforementioned dispersion coefficients were within the range of the derived sediment-based coefficient without applying the layer-based factor (blue columns in Figure 10b). The transverse dispersivity in the model was applied as 0.5 m.

In addition to dispersivity, porosity is another critical parameter influencing salinity transport in groundwater systems. In this study, a uniform effective porosity value of 0.3 was applied to both aquifers and aquitards. This choice aligns with values commonly reported for sandy aquifers [58,59] and is consistent with previous regional-scale groundwater models in the Mekong Delta, which typically adopted effective porosity values in the range of 0.25–0.30 without differentiating between aquifers and aquitards [6,13,26]. Although some studies, such as [35], assigned distinct porosity values to aquifers and aquitards based on the sediment type, the application of a single representative value remains a common and acceptable simplification in large-scale models aiming for consistency and tractability.

We acknowledge, however, that the effective porosity of aquitard materials such as clay is generally lower, typically ranging from 0.01 to 0.18 [60,61]. Nevertheless, as our model focuses primarily on horizontal transport processes in sandy aquifers, the impact of this simplification on the overall salinity distribution is expected to be limited. Future studies may benefit from implementing spatially variable porosity fields derived from detailed

lithological data to better capture vertical transport and retardation effects, particularly in fine-grained aquitard layers.

4.3. Limitations of the Model

In order to evaluate the groundwater salinization processes in the CMP, the model was adapted accordingly based on the available dataset. However, the model incorporates some limitations due to the limited available data.

No private household wells are included in the model, since household wells operate with very small flows. Instead, the water consumption for each commune is based on the population and an average rural water demand of 34 L/person/day [12]. This water consumption for each commune is implemented in the model by several wells with a total flow rate equivalent to the derived water demand. With this method, the assumed amount of the water extraction by a large number of private household wells is represented by fewer wells in the model.

The drilling time of wells is not considered during the transient model calculation: all wells are included in the model throughout the whole calculation period. However, in reality, many of the deeper wells are drilled later than the shallow wells. This time dependency could be considered in further evaluations.

Additionally, the use of a spatially uniform effective porosity value for both aquifers and aquitards, while consistent with several previous regional studies, may not fully represent the heterogeneity of fine-grained aquitard layers and their limited contribution to advective transport. Furthermore, the use of uniform porosity values may underestimate the effects of fine-scale heterogeneities, which are especially relevant in layered systems.

5. Salinity Model Results

The groundwater flow model validation was discussed in detail in [12]; thus, the following discussion focuses on the aspects of the transport model only. The longitudinal dispersivity parameters of the transport model are not calibrated. They have been estimated by a regionalized method using representative literature values and correction methods. According to the described validation criteria, salinity modeling can be performed for the purposes of confidence building and scientific validation. As stated by Ref. [62], confidence building “is a measure of the adequacy of the model structure (conceptual model and mathematical model) in describing the system behavior” and “is a measure of the accuracy of the model input parameters relative to experimental results and field observations”. For regional validation at different time steps, the scientific view postulated by [63] demands the validation of specific models “that one might reasonably expect someone with relevant technical knowledge to consider the model acceptable”.

As described in the Data Collection Section, there are only very limited continuous salinity data available that could be used for a transient model calibration. Therefore, as an alternative approach, the comparison of measured and modeled salinity concentrations was used to validate the implemented salinization processes and assess their relevance. In Figure 11, the values measured twice a year, as well as the modeled TDS concentrations, for different aquifers are shown as time series.

Figure 11 illustrates that the modeled TDS concentrations at the presented monitoring wells align closely with the observed values, both in terms of magnitude and temporal trends. The modeled salinity concentrations at monitoring well Q199 qh (Figure 11a) show seasonal variations as a result of the applied boundary conditions with interannual variations (as shown in Figure 8). This indicates that part of the measured variability may be caused by the interannual variation in salinity assumed in the rivers system. Thus, we identify this process as a potential contributor to the salinization pathway, but other

impacts on the variability remain unclear. This can also be observed in Figure 11b for well Q177 qh, where the model simulates the general trend well but the observed variations in the TDS concentrations are not reflected, indicating that a further consideration of locations with interannual variations in the TDS boundary conditions in qh could improve the model results, such as the Q177 site, where constant TDS boundary conditions are applied.

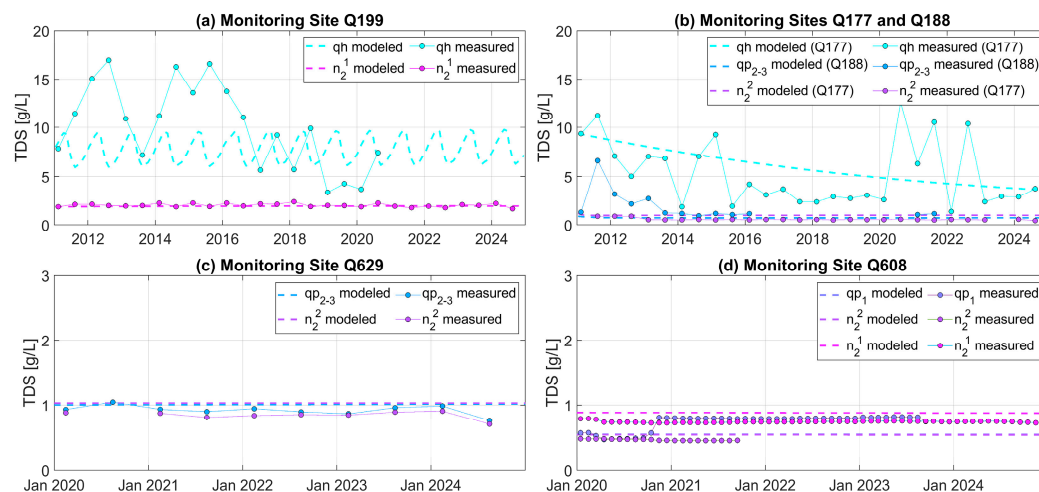


Figure 11. Time-dependent comparison of measured and modeled salinity for different well groups and aquifers. (a) Q199 (qh)—Seasonal and interannual variation captured; (b) Q177 (qh)—General trend matched; short-term variability not reproduced; (c) Q629 (qp₂₋₃, n₂)—Stable salinity indicates limited vertical transport; and (d) Q608 (deep)—Consistent salinity primarily driven by initial conditions.

Figure 11c (monitoring site Q629) shows a more stable trend in the observed and modeled TDS concentrations for the aquifer layers qp₂₋₃ and n₂². The model captures the general trend, with slight deviations observed during the period from 2020 to 2024. This consistency suggests that vertical transport processes in deeper aquifers may be limited or occur at a much slower rate. However, minor discrepancies, especially near the end of the time series, may still arise from sampling conditions, laboratory handling, or other external influences that require further investigation.

The salinity in the deeper aquifers qp₁ and n₂² tends to be stable in the monitoring wells, without interannual variation. Figure 11a–d show that the simulated (Q199, Q188, Q177, Q629, and Q608) TDS concentrations effectively depict the behavior of the groundwater system over an extended validation period (from 2011 to 2024) in the complex exploitation setting. This indicates that only the initial condition is responsible for the well-simulated salinity in the deeper aquifers. It also suggests that during this extended period, the vertical transport of salinity remains very slow, further confirming the stability observed in deeper aquifer systems.

A common method for evaluating model performance in groundwater modeling is through scatterplots. Figure 12 presents the scatterplot comparing modeled and measured TDS concentrations at observation wells during various time intervals from 2011 to 2024. The 1:1 line represents a perfect agreement between modeled and measured values, while the $\pm 10\%$ and $\pm 20\%$ boundaries highlight regions of underestimation or overestimation by the model. This scatterplot offers a qualitative assessment of the model's performance.

It is important to note that the larger discrepancies seen in Figure 12 are primarily associated with observation wells located in the shallow aquifer (qh), which were deliberately separated from other wells for targeted evaluation. This is due to the high seasonal variability and surface influence affecting TDS concentrations in qh, particularly given the model's reliance on land use data to estimate the recharge salinity in these shallow zones.

In contrast, wells in deeper aquifers show a much closer match to observed values, with the majority falling within the $\pm 10\%$ or $\pm 20\%$ deviation bands. This distinction highlights both the complexity of modeling shallow systems and the overall robustness of the model in representing deeper groundwater salinization processes. Despite some discrepancies in absolute values in qh, as observed in Figure 11a,b, the model effectively captured the overall trends and variability in the TDS at the shallow aquifer level.

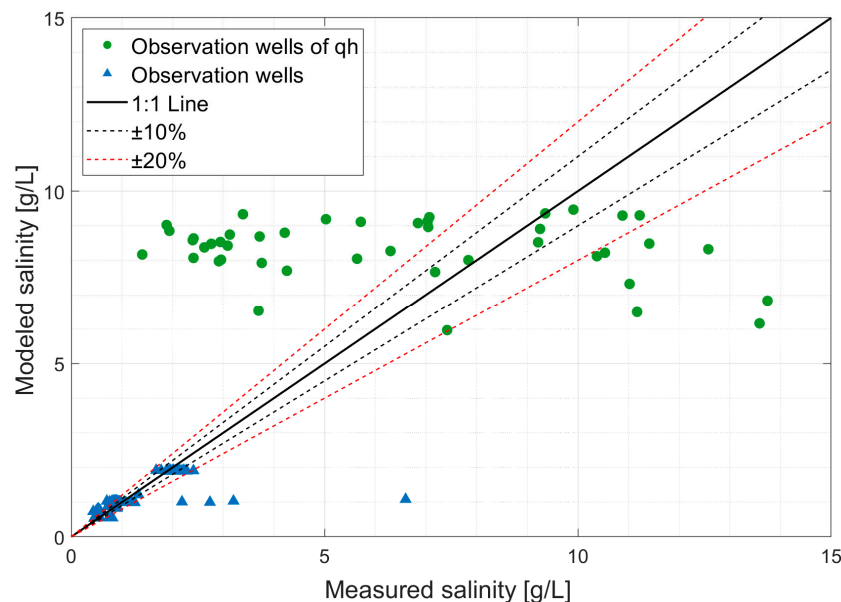


Figure 12. A comparison between measured versus modeled average TDS concentrations (g/L) at observation wells during the simulation period (2011–2024). The solid black line represents a perfect 1:1 match, while dashed lines indicate $\pm 10\%$ and $\pm 20\%$ deviations. Green circles represent qh wells affected by surface processes and land use variability, while blue triangles indicate deeper aquifers with a generally closer agreement.

The salinity distribution in January 2011 served as the initial conditions for aquifers qh and qp₃, as outlined in the Section Initial Conditions. Subsequent simulations captured changes in the TDS concentrations, with Figure 13 providing a visual representation of these variations. In the top-right portion of Figure 13, the influence of the boundary conditions with interannual variations is evident, resulting in a reduction in the salinity of the qh aquifer during the rainy season. This reduction is likely attributed to the dilution caused by the influx of freshwater from precipitation events. Conversely, for August 2022, the bottom-right portion of Figure 13 illustrates an increase in salinity in aquifer qp₃. This increase is attributed to the substantial transport of salinity from aquifer qh to qp₃. Furthermore, the long-term simulation uncovered additional dynamics in the salinity distribution. In the top-right portion of Figure 13, there is an indication of salinity import from the top, possibly influenced by external factors or processes affecting the upper part of the aquifer. Simultaneously, the bottom-right portion shows ongoing salinity transport from the top down, suggesting the continuous downward movement of saline water within the aquifer system.

Figure 13 shows that the salinity transport was dominated by input from the surface, and the modeled salinity in the two upper aquifers qh and qp₃ shows a strong change over the simulation between January 2011 and August 2022. In contrast, the lower aquifers qp₂₋₃ and n₂² show fewer changes in salinity over time (for comparison, see two lower maps in Figure 14a–e). The scale is defined within an interval of 1.0 g/L. For the deeper aquifers qp₂₋₃ and n₂² (Figure 14a–e), no significant lateral change in salinity can be obtained from the model results for the simulation period. In the current model described above, only a

small-scale variation in salinity due to pumping can be detected. However, this is consistent with the time series measurement of the salinity, as no significant changes in salinity over time could be observed (see Figure 11). Figure 14c,f show the modeled spatial changes in the freshwater zones (<1 g/L) between 2011 and 2022. Both time steps include the 1 g/L isolines to allow the direct comparison of the salinity extent between 2011 and 2022. In qp₂₋₃ (Figure 14c), region 1 shows an increase in salinity along the border of the original salinity inflow from the ocean, while region 2 presents a northward expansion of salinity from the northern boundary (Bac Lieu Province), likely induced by intensive groundwater extraction. In regions 3 and 4, salinity levels exceed 1 g/L due to the lateral transport of brackish water, rendering the groundwater unsuitable for drinking. In aquifer n₂² (Figure 14f), changes are less pronounced, but a local increase in salinity is noticeable in the eastern parts (regions 5 and 6), following the direction of the horizontal groundwater flow.

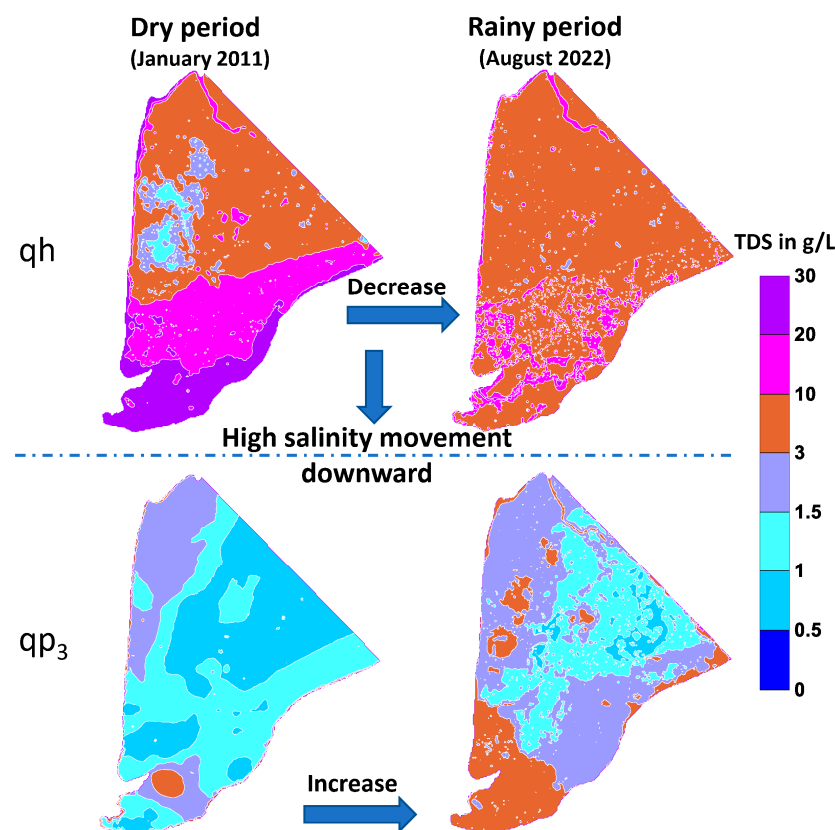


Figure 13. The modeled salinity distribution (TDS in g/L) in aquifers qh and qp₃ during the dry period (January 2011) and the rainy period (August 2022).

These patterns of lateral salinity increase—particularly in the northeast (Bac Lieu) and west—may reflect the influence of anisotropic aquifer properties, where a horizontal hydraulic conductivity dominates. In the Mekong Delta’s stratified aquifer systems, interbedded clay or silt layers tend to impede vertical flow while allowing horizontal movement. This likely limits the downward salt transport from qp₃ to deeper units like qp₂₋₃ and n₂², despite pumping activity. However, due to the coarse resolution of the model, such anisotropic behavior is not explicitly represented.

In the southern part of the CMP, the model also indicates vertical salinity transport from qp₃ to qp₂₋₃, originating from the mangrove regions in the upper layers (Figure 9). As a result of the model, we only observe small influences on the vertical salinity movement in qp₂₋₃ and n₂², which result from pumping. Exploitation is simulated based on area-wide values rather than specific points. In regions with high pumping rates, such as Ca Mau City,

the results therefore suggest a stable salinity as compared to other regions, as illustrated in Figure 14d,e.

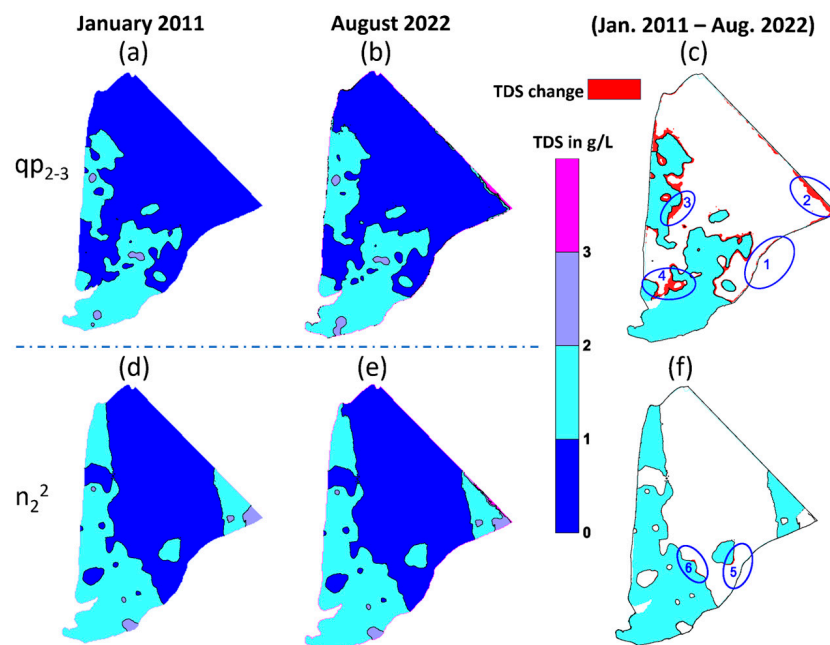


Figure 14. The development of the salinity from 2011 up to 2022 for aquifer qp₂₋₃ (a,b) and n₂² (d,e); (c,f) illustrate the difference between simulation results from 2011 to 2022.

In the study by [22] it was found, among 144 participants who completed questionnaires in Ca Mau, that the percentage of exploited groundwater allocated for cooking purposes constituted 65.7% of the water usage, while 97% of respondents used groundwater for washing purposes. These freshwater areas are depicted as dark-blue regions in Figure 14a,b, representing the northeastern Ca Mau Province. In the future, the number of areas with higher salinity is likely to increase due to similar pumping-induced effects, as illustrated in Figure 14c. Thus, the possibility of pumping freshwater from qp₂₋₃ will decrease. In this area, freshwater has to be substituted from other sources, such as rain-water harvesting or water diversion structures from other sites. In regions with brackish groundwater, with a salinity exceeding 1 g/L but below 3 g/L, it will be possible to use water from the qp₂₋₃ aquifer for cleaning and washing in the near future.

For aquifer n₂² (Figure 14d,e), the model showed a local increase in the saline water area in the east from January 2011 to August 2022 (Figure 14f, red color), due to the horizontal salinity movement along the direction of the groundwater flow.

6. Discussion

6.1. Key Controls on Salinity Dynamics

As previously mentioned in the Methodology Section, our approach was primarily exploratory, aiming to elucidate dominant physical mechanisms rather than achieving a perfect fit to limited observational data.

The complex interaction between surface water salinity and the upper aquifer qh in the CMP remains inadequately characterized, despite its importance for regional water management. Elevated salinity concentrations in both sediments and water bodies are a ubiquitous problem in the CMP. The salinity varies at the local scale (5–10 m), but the relative effects of land use and surface geology on the salinity variation in the near-surface zone (<5 m) are still unclear. Reference [64] identified that “the influence of surface water salinity (associated with different land uses) on the groundwater salinity regime is

pervasive". They found that areas underlying a shrimp farm/tidal flat displayed a higher salinity regardless of the near-surface sediment characteristics, while areas underlying drinking water ponds or inhabited areas had a relatively low salinity. In this study, the impact of land use and the infiltration of surface water into the qh aquifer was implemented in a numeric model to simulate the relationship between land use and groundwater salinity.

In addition to the spatial variability driven by land use patterns, temporal variations in salinity also present significant complexity, particularly in the shallow aquifer system. Our analysis indicated that significant fluctuations primarily occurred within the shallow qh aquifer, which were strongly influenced by seasonal factors and surface activities such as irrigation, aquaculture, and the tidal-induced salinity intrusion through rivers and canals. Deeper aquifers generally exhibited stable salinity trends both in observational data and model simulations. However, our model also revealed localized temporal variations at certain production wells, where increasing or decreasing trends in TDS were observed (as explicitly presented in Figure 15). These findings underscore the complexity of groundwater salinity dynamics, which are driven by both natural hydrological processes and anthropogenic activities. Beyond surface-driven influences, the internal structure and connectivity of the aquifer system also play a crucial role in shaping salinity behavior.

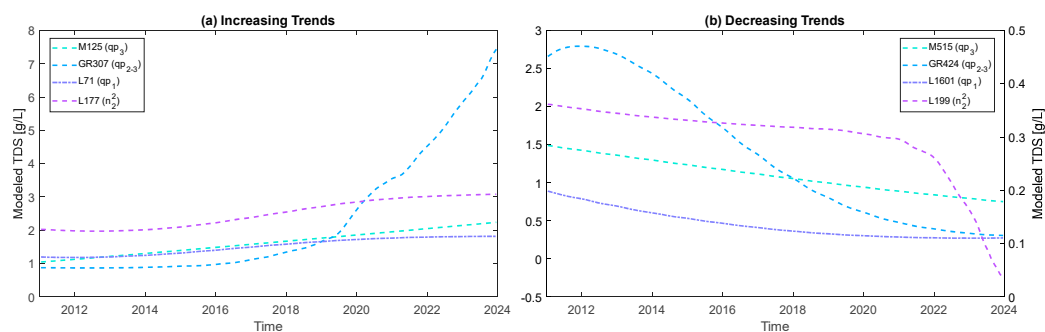


Figure 15. Modeled TDS variations at selected wells across aquifers (2011–2024) (upper Pleistocene—qp₃; Upper–Middle Pleistocene—qp_{2–3}; Middle Pliocene—n₂²; and Lower Pliocene—n₂¹); see Figure 3 (source of data: NAWAPI).

Other key factors influencing salinity dynamics are geological heterogeneity and anisotropy. Variations in hydraulic conductivity, the presence of semi-permeable aquitards, and preferential flow paths across layers may significantly influence saltwater migration patterns. These physical features, combined with anthropogenic stresses such as intensive groundwater abstraction, can alter vertical and lateral salinity gradients. In multi-aquifer systems like Ca Mau, long-term pumping can enhance inter-aquifer leakage, mobilizing deeper or trapped paleo-saline water towards abstraction zones. Consistent with this, ref. [65] demonstrated through numerical modeling that the presence of preferential flow pathways in heterogeneous aquifers significantly accelerates saltwater intrusion processes under groundwater pumping conditions, emphasizing the combined impact of geological heterogeneity and human-induced stresses.

However, a detailed quantitative assessment of individual parameters, such as the hydraulic conductivity, porosity, and geological structure, was beyond the scope of this exploratory study. In addition, due to the coarse spatial resolution of the regional-scale model, preferential flow processes were not explicitly resolved. These mechanisms are often better captured in high-resolution 2D or localized 3D models. For instance, [65] illustrated the influence of preferential flow on pumping-induced salinity intrusion using a focused modeling approach. Future research should aim to combine detailed vertical salinity analyses, parameter sensitivity assessments, and high-resolution subregional models to

better quantify the roles of aquifer heterogeneity, anisotropy, and preferential pathways in salinity dynamics across the CMP.

6.2. Model Representation and Applicability

As shown in the scatterplot (Figure 12), the modeled salinity values generally align well with the measured data. However, discrepancies are evident, particularly in the qh aquifer, where the errors are more pronounced. These deviations suggest that while the model effectively captures general trends, it does not accurately replicate localized variations in salinity. This limitation can be attributed to the scarcity of detailed observational data for the upper layer, regionalized longitudinal dispersivity parameters, and potential unknown local factors that remain beyond the scope of the current model.

Interannual variations in the TDS concentrations at observation wells are most evident for the qh aquifer. Nevertheless, even in deep aquifers (e.g., in n_2^1 at Q199 (Figure 11a)), such interannual variations are observed. In order to model these dynamics, interannually variable TDS boundary conditions were applied at selected locations in the model for the qh aquifer. Nonetheless, these dynamics in the TDS concentration did not propagate to the lower aquifers in a sufficient magnitude in the model.

To address this, the model's intent is not to focus on the detailed representation of the uppermost layer but to propose a conceptual framework. This framework leverages land use maps with varying salinity levels for the surface layer, combined with seasonal salinity variations, to simulate broader regional patterns effectively. Such an approach is a pragmatic solution for a wide-scale analysis, especially when high-resolution data are unavailable.

As highlighted by ref. [64], the distance from rivers can influence groundwater salinity, but the presence of saline water within the rivers themselves often plays a more significant role. Their study identified that areas located approximately 400–500 m from rivers exhibited groundwater salinity levels ranging from 2.8 to 3.8 g/L (4100–5500 $\mu\text{S}/\text{cm}$, with a conversion factor EC to TDS of $k = 0.7$). In this study, we observed similar patterns at well Q199010 in the qh aquifer, where interannual salinity levels varied between 6 and 10 g/L (Figure 9, top left). This well, located approximately 100 m from the nearest river, experiences a significant influence from the tidal system and seasonal variations, including rainy and dry periods. The modeled interannual variability in the TDS at this location (4–8 g/L, as shown by the green dashed line in Figure 11a) aligns closely with Rahman et al.'s observations, reinforcing the critical role of river proximity and tidal influences in shaping groundwater salinity dynamics.

6.3. Management Strategies and Research Priorities

Effective groundwater salinity management requires a nuanced understanding of both regional and local dynamics. In this context, Figure 15 below illustrates modeled TDS variations across selected representative wells, helping to visualize localized salinity trends across aquifers. For these wells, salinity increases when pumping induces the movement of saline water from the surrounding areas toward the well due to a steeper hydraulic gradient. Conversely, salinity decreases where freshwater inflow dominates, diluting the salinity in the pumping wells. These localized trends reflect the complexity of salinity dynamics, driven by the interplay between groundwater exploitation, hydrogeological conditions, and the spatial distribution of freshwater and saline water lenses. Field surveys further confirmed that these changes align with the influence of paleowater mixing and extraction-induced hydraulic gradients, emphasizing the need to consider ancient trapped saline water in evaluating long-term salinization risks.

Additionally, Figure 15 demonstrates that among the 1101 pumping wells in the model, salinity fluctuations—both increases and decreases—are observed at many locations, depending on local conditions. These dynamics emphasize the need for site-specific strategies to effectively manage groundwater resources in areas impacted by saltwater intrusion. Such strategies should consider localized variations and the broader regional dynamics to ensure sustainable groundwater use.

Moreover, data resolution plays a crucial role in shaping the observed salinity patterns. According to the ref. [23], salinity maps with higher point densities—such as in the qp₂₋₃ aquifer—exhibited greater spatial complexity compared to deeper aquifers like n₂¹, where fewer data points were available. This suggests that some apparent homogeneity may result from data scarcity rather than actual aquifer uniformity. The report recommends acquiring at least 50 spatially distributed sampling points per aquifer for provinces with areas exceeding 5000 km². Implementing such monitoring strategies would enhance our ability to characterize heterogeneity and improve model reliability for groundwater salinization assessments.

Based on the criteria detailed in Section 4.2.2, the system's salinization behavior is reasonably well represented in the model from a confidence-building perspective. The calculated salinity was validated against point-measured data, with the simulated results showing a reasonable agreement in terms of magnitude and temporal evolution. This aligns with the operational aspect of model validation, i.e., “that a good, correct, or sufficient representation of reality” in time and space can be achieved with the model. Moreover, the model can be considered acceptable as it incorporates knowledge of the hydrogeological and salinity context in the CMP for its setup.

Ref. [66] obtained salinity forecasts covering the period up to 2026, focusing on a 1.5 g/L shift (below 1.5 g/L and above 1.5 g/L) in the saline boundary line in two different regions. The work described in this study presents a salinity distribution with improved detail. Due to the initialization dataset used for each aquifer, more monitoring data would be needed for a more accurate salinity forecast model. Our model indicated that the salinity movement in the deeper aquifers appeared to be slow, which is consistent with the predictions made by ref. [66].

As illustrated in the cross-section in Figure 3, the aquitard thicknesses vary significantly in the southernmost region of the MKD. This variation in thickness, along with the small number of available drilling logs upon which the layer interpolation is based, can be considered an indicator that hydrogeological windows may indeed exist in different aquitards, even though they have not yet been identified in drilling logs. This observation points to the need for further investigation into the potential salinization pathways in this area.

Building on this finding, as neither the observed TDS concentrations in the monitoring wells nor the modeled concentrations showed a significant increase in salinity during the simulation period from 2011 to 2024, it becomes evident that further potential pathways of groundwater salinization need to be evaluated. To achieve this, a sensitivity analysis of the vertical hydraulic conductivity interaction between the aquifers should be conducted to better understand the dynamics of salinity movement.

Further an investigation regarding the comparison of the TDS concentrations of monitoring wells, active production wells, and abandoned production wells is necessary to better understand the impact of pumping and well construction on the local groundwater salinity.

7. Conclusions

Building on the groundwater flow model of [12], this study developed an enhanced 3D density-dependent transport model to investigate the understanding of saltwater dynamics

and salinization processes in the CMP. The model incorporated new approaches, including the determination of longitudinal dispersivity as a function of sediment type and the inclusion of interannual salinity impacts driven by land use, infiltration from river systems, and mangrove areas.

These advancements enabled the detailed identification of high-salinity regions in aquifer qh and their influence on the salinity dynamics in qp₃ and parts of qp_{2–3}. The deeper aquifers predominantly contained freshwater (TDS below 1.0 g/L) with a minimal temporal variation over the analyzed timeframe (2011–2024). However, localized regions in northeast Ca Mau (Bac Lieu) exhibited higher salinity, highlighting potential pathways of salinization through hydrological windows or lateral flow.

Notably, the model results showed a fair correlation between simulated and measured salinity values across different aquifers, validating its reliability in capturing broad salinity trends. The surface salinization from various land use types significantly impacted the qh aquifer, while deeper layers did not exhibit clear top-down salinization trends during the observed period.

Although monitoring wells did not show a clear increase in salinity, the model demonstrated that, based on the analysis of production wells, localized salinity increases were evident in areas impacted by groundwater extraction.

This study confirms that land use-related salinity inputs significantly affect the shallow aquifer, while deeper aquifers remain relatively stable. Model outputs aligned with field observations, indicating the effectiveness of the approach in representing salinization trends across aquifers.

Overall, this study contributes to a nuanced understanding of salinity intrusion pathways and provides valuable insights for managing groundwater resources in regions affected by saltwater intrusion.

Author Contributions: Conceptualization, T.V.H., S.N., K.-G.R. and F.D.; methodology, T.V.H., K.-G.R., F.D. and J.B.; validation, formal analysis, and investigation, T.V.H. and K.-G.R.; resources, V.T.M.L., A.S., N.B. and S.N.; writing—original draft preparation, T.V.H. and K.-G.R.; writing—review and editing, T.V.H., F.D., K.-G.R., J.B., N.B., A.S., V.T.M.L., V.C.P., D.V.T. and S.N.; supervision, S.N.; funding acquisition, S.N.; administrator, S.N. and N.B. All authors have read and agreed to the published version of the manuscript.

Funding: This study was funded by the Karlsruhe Institute of Technology; This work is part ViWaT – Engineering project, funded by the German Ministry of Education and Research (BMBF) under grant No. 02WCL1474A; and the Catholic Academic Exchange Service (KAAD).

Data Availability Statement: The data described in this paper are available upon request to the corresponding author. A permission letter was obtained from the NAWAPI for the collection of the rainfall data, groundwater quality data, surface- and groundwater-level data, and water exploitation data.

Acknowledgments: This paper benefitted substantially from the comments and suggestions of the two anonymous reviewers. This publication was supported by the Publication Fund of the Karlsruhe Institute of Technology, the German Ministry of Education and Research (BMBF), the ViWaT Engineering research project, the Ministry of Science and Technology (MOST), and the Catholic Academic Exchange Service (KAAD). This work is was contribution to German– Vietnamese research initiative ViWaT Mekong (<http://www.viwat.info/english/21.php> (accessed on 25 April 2025)).

Conflicts of Interest: Author Karl-Gerd Richter was employed by the company Aquantec Company for Water and Environment GmbH. The remaining authors declare that the research was conducted in the absence of any commercial or financial relationships that could be construed as a potential conflict of interest.

References

- Ha, Q.K.; Dang, V.T.; Vo, L.P.; Dang, D.H. Integrated approaches to track saline intrusion for fresh groundwater resource protection in mekong delta. *Groundw. Sustain. Dev.* **2023**, *23*, 101046. [CrossRef]
- Michael, H.A.; Post, V.E.A.; Wilson, A.M.; Werner, A.D. Science, society, and the coastal groundwater squeeze. *Water Resour. Res.* **2017**, *53*, 2610–2617. [CrossRef]
- Post, V.E.A.; Groen, J.; Kooi, H.; Person, M.; Ge, S.; Edmunds, W.M. Offshore fresh groundwater reserves as a global phenomenon. *Nature* **2013**, *504*, 71–78. [CrossRef] [PubMed]
- Werner, A.D.; Bakker, M.; Post, V.E.A.; Vandenbohede, A.; Lu, C.; Ataie-Ashtiani, B.; Simmons, C.T.; Barry, D.A. Seawater intrusion processes, investigation and management: Recent advances and future challenges. *Adv. Water Resour.* **2013**, *51*, 3–26. [CrossRef]
- Ferguson, G.; Gleeson, T. Vulnerability of coastal aquifers to groundwater use and climate change. *Nat. Clim. Change* **2012**, *2*, 342–345. [CrossRef]
- Minderhoud, P.S.J.; Erkens, G.; Pham, V.H.; Bui, V.T.; Erban, L.; Kooi, H.; Stouthamer, E. Impacts of 25 years of groundwater extraction on subsidence in the Mekong delta, Vietnam. *Environ. Res. Lett.* **2017**, *12*, 064006. [CrossRef]
- Custodio, E. Coastal aquifers of Europe: An overview. *Hydrogeol. J.* **2010**, *18*, 269–280. [CrossRef]
- UN VIETNAM. Viet Nam Drought and Saltwater Intrusion in the Mekong Delta. Joint Assessment Report. January, 15–17. 2020. Available online: https://reliefweb.int/sites/reliefweb.int/files/resources/MekongDeltaDroughandSaltwaterIntrusion_JointAssessmentReport_Feb2020.pdf (accessed on 10 June 2024).
- Bauer, J.; Börsig, N.; Pham, V.C.; Hoan, T.V.; Nguyen, H.T.; Norra, S. Geochemistry and evolution of groundwater resources in the context of salinization and freshening in the southernmost Mekong Delta, Vietnam. *J. Hydrol. Reg. Stud.* **2022**, *40*, 101010. [CrossRef]
- Allison, M.A.; Nittrouer, C.A.; Ogston, A.S.; Mullarney, J.C.; Nguyen, T.T. Sedimentation and survival of the Mekong delta: A case study of decreased sediment supply and accelerating rates of relative sea level rise. *Oceanography* **2017**, *30*, 98–109. [CrossRef]
- Van Binh, D.; Kantoush, S.; Sumi, T. Changes to long-term discharge and sediment loads in the Vietnamese Mekong Delta caused by upstream dams. *Geomorphology* **2020**, *353*, 107011. [CrossRef]
- Hoan, T.V.; Richter, K.G.; Börsig, N.; Bauer, J.; Ha, N.T.; Norra, S. An Improved Groundwater Model Framework for Aquifer Structures of the Quaternary-Formed Sediment Body in the Southernmost Parts of the Mekong Delta, Vietnam. *Hydrology* **2022**, *9*, 61. [CrossRef]
- Vuong, B.T.; Chan, N.D.; Nam, L.H.; Bach, T.V.; Long, P.N.; Van Hung, P. Report on Construction of Model of Groundwater Flow and Models of Saline–Fresh Groundwater Interface Movement for Mekong Delta (Issue 434); 2014. Available online: https://www.researchgate.net/publication/375642932_The_Process_of_Groundwater_Salinization_on_the_Ca_Mau_Peninsula_Mekong_Delta_Vietnam_Evaluation_of_Saltwater_Intrusion_Pathways_via_Scenario_Calculations_Applying_a_3D_Groundwater_Model/fulltext/6554b793b86a1d521be6c0af/The-Process-of-Groundwater-Salinization-on-the-Ca-Mau-Peninsula-Mekong-Delta-Vietnam-Evaluation-of-Saltwater-Intrusion-Pathways-via-Scenario-Calculations-Applying-a-3D-Groundwater-Model.pdf (accessed on 10 May 2025).
- Wagner, F.; Tran, V.B.; Renaud, F.G. Groundwater Resources in the Mekong Delta: Availability, Utilization and Risks. In *The Mekong Delta System*; Springer: Dordrecht, The Netherlands, 2012. [CrossRef]
- Burgess, W.G.; Shamsudduha, M.; Taylor, R.G.; Zahid, A.; Ahmed, K.M.; Mukherjee, A.; Lapworth, D.J.; Bense, V.F. Terrestrial water load and groundwater fluctuation in the Bengal Basin. *Sci. Rep.* **2017**, *7*, 3872. [CrossRef] [PubMed]
- Van Hoang, H.; Larsen, F.; Van Lam, N.; Nhan, D.D.; Luu, T.T.; Nhan, P.Q. Salt Groundwater Intrusion in the Pleistocene Aquifer in the Southern Part of the Red River Delta, Vietnam. *VNU J. Sci. Earth Environ. Sci.* **2018**, *34*, 10–22. [CrossRef]
- Jusseret, S.; Tam, V.T.; Dassargues, A. Groundwater flow modelling in the central zone of Hanoi, Vietnam. *Hydrogeol. J.* **2009**, *17*, 915–934. [CrossRef]
- Lam, Q.D.; Meon, G.; Pätsch, M. Coupled modelling approach to assess effects of climate change on a coastal groundwater system. *Groundw. Sustain. Dev.* **2021**, *14*, 100633. [CrossRef]
- Minderhoud, P.S.J.; Middelkoop, H.; Erkens, G.; Stouthamer, E. Groundwater extraction may drown mega-delta: Projections of extraction-induced subsidence and elevation of the Mekong delta for the 21st century. *Environ. Res. Commun.* **2020**, *2*, 011005. [CrossRef]
- Nam, N.D.G.; Goto, A.; Osawa, K.; Ngan, N.V.C. Modeling for analyzing effects of groundwater pumping in Can Tho city, Vietnam. *Low. Technol. Int.* **2019**, *21*, 33–43.
- Harbaugh, A.W. MODFLOW-2005, The U.S. Geological Survey Modular Ground-Water Model—the Ground-Water Flow Process MODFLOW-2005; US Geological Survey: Reston, VI, USA, 2005. [CrossRef]

22. Pham, V.C.; Bauer, J.; Börsig, N.; Ho, J.; Vu, L.; Tran, H.; Dörr, F.; Norra, S. Groundwater Use Habits and Environmental Awareness in Ca Mau Province, Vietnam: Implications for Sustainable Water Resource Management. *Environ. Chall.* **2023**, *13*, 100742. [CrossRef]
23. Manh, L.V.; Steinel, A. *Groundwater Salinity Distribution Mapping for Ca Mau Province*; Technical Note TN-IV-03. Technical Note TN-IV-03. 'Improvement of Groundwater Protection in Vietnam (IGPVN)' Project, Hanoi, Vietnam; National Center for Water Resources Planning and Investigation (NAWAPI), Vietnam & Federal Institute for Geosciences and Natural Resources (BGR): Koblenz, Germany, 2021; p. 63.
24. Li, D.; Long, D.; Zhao, J.; Lu, H.; Hong, Y. Observed changes in flow regimes in the Mekong River basin. *J. Hydrol.* **2017**, *551*, 217–232. [CrossRef]
25. Minderhoud, P.S.J.; Coumou, L.; Erkens, G.; Middelkoop, H.; Stouthamer, E. Mekong delta much lower than previously assumed in sea-level rise impact assessments. *Nat. Commun.* **2019**, *10*, 3847. [CrossRef]
26. Pham, V.H.; Van Geer, F.C.; Bui Tran, V.; Dubelaar, W.; Oude Essink, G.H.P. Paleo-hydrogeological reconstruction of the fresh-saline groundwater distribution in the Vietnamese Mekong Delta since the late Pleistocene. *J. Hydrol. Reg. Stud.* **2019**, *23*, 100594. [CrossRef]
27. Hoanh, C.T.; Phong, N.D.; Gowing, J.W.; Tuong, T.P.; Ngoc, N.V.; Hien, N.X. Hydraulic and water quality modeling: A tool for managing land use conflicts in inland coastal zones. *Water Policy* **2009**, *11* (Suppl. S1), 106–120. [CrossRef]
28. Duong, T.D.; Vo, V.T.; Pham, M.T.; Cuong Kien, D. Dự Báo đỉnh Mặn Tại Các Trạm Đo Chính Của Tỉnh Cà Mau Bằng Mô Hình Chuỗi Thời Gian Mờ. 2016. Available online: <https://ctujsvn.ctu.edu.vn/index.php/ctujsvn/article/view/2508> (accessed on 20 December 2024).
29. Le Duy, N.; Nguyen, T.V.K.; Nguyen, D.V.; Tran, A.T.; Nguyen, H.T.; Heidbüchel, I.; Merz, B.; Apel, H. Groundwater dynamics in the Vietnamese Mekong Delta: Trends, memory effects, and response times. *J. Hydrol. Reg. Stud.* **2021**, *33*, 100746. [CrossRef]
30. Doan, V.C.; Dang, D.N.; Nguyen, K.C. Formation and chemistry of the groundwater resource in the Mekong river delta, South Vietnam. *Vietnam J. Sci. Technol. Eng.* **2018**, *60*, 57–67. [CrossRef]
31. NAWAPI. *Bulletins Announcing, Forecasting and Warning Water Resources in the Mekong River Basin*; National Center for Water Resources Planning and Investigation (NAWAPI): Hanoi, Vietnam, 2024.
32. Ha, Q.K.; Tran Ngoc, T.D.; Le Vo, P.; Nguyen, H.Q.; Dang, D.H. Groundwater in Southern Vietnam: Understanding geochemical processes to better preserve the critical water resource. *Sci. Total Environ.* **2022**, *807*, 151345. [CrossRef]
33. Barcelona, M.J.; Wehrhaann, H.A.; Varljen, M.D. Reproducible Well-Purging Procedures and VOC Stabilization Criteria for Ground-Water Sampling. *Groundwater* **1994**, *32*, 12–22. [CrossRef]
34. Nielsen, D.M.; Nielsen, G. *The Essential Handbook of Ground-Water Sampling*; CRC Press: Boca Raton, FL, USA, 2006. [CrossRef]
35. Gunnink, J.; Van Pham, H.; Oude Essink, G.; Bierkens, M. The 3D groundwater salinity distribution and fresh groundwater volumes in the Mekong Delta, Vietnam, inferred from geostatistical analyses. *Earth Syst. Sci. Data Discuss.* **2021**, *13*, 3297–3319. [CrossRef]
36. Cressie, N.A.C. Statistics for Spatial Data Revised edition. In *Statistics for Spatial Data*; John Wiley & Sons, Inc.: Hoboken, NJ, USA, 2015; pp. 1–900. [CrossRef]
37. DHI-WASY GmbH. FEFLOW 7.2. 2022. Available online: <https://www.mikepoweredbydhi.com/products/feflow> (accessed on 20 January 2025).
38. Monre. *Socialist Republic of Vietnam, Technical Regulations for Mapping Groundwater Quality, Scale 1:25,000. 08/2014/TT-BTNMT (Translated)*; Ministry of Natural Resources and Environment: Hanoi, Vietnam, 2014; pp. 20–37.
39. Wehrheim, C.; Lübken, M.; Stolpe, H.; Wichern, M. Identifying key influences on surface water quality in freshwater areas of the Vietnamese Mekong Delta from 2018 to 2020. *Water* **2023**, *15*, 1295. [CrossRef]
40. Bear, J.; Verruijt, A. Modeling Groundwater Pollution. In *Modeling Groundwater Flow and Pollution*; Springer: Dordrecht, The Netherlands, 1987; pp. 153–195. [CrossRef]
41. Grathwohl, P. Diffusion in Natural Porous Media: Contaminant Transport, Sorption/Desorption and Dissolution Kinetics. 1998. Available online: <http://www.springer.com/earth+sciences+and+geography/book/978-0-7923-8102-0> (accessed on 15 January 2025).
42. Jacques, W.D. *The Handbook of Groundwater Engineering*, 2nd ed.; T. & F. Group, Ed.; CRC Press: Boca Raton, FL, USA, 2019.
43. Koch, D.L.; Brady, J.F. A Non Local Description of Advection-Diffusion With Application to Dispersion in Porous Media. *J. Fluid Mech.* **1987**, *180*, 387–403. [CrossRef]
44. Al-Tabbaa, A.; Ayotamuno, J.M.; Martin, R.J. One-dimensional solute transport in stratified sands at short travel distances. *J. Hazard. Mater.* **2000**, *73*, 1–15. [CrossRef]
45. Leij, F.J.; Van Genuchten, M.T. Approximate analytical solutions for solute transport in two-layer porous media. *Transp. Porous Media* **1995**, *18*, 65–85. [CrossRef]
46. Sternberg, S.P.K. Dispersion Measurements in Highly Heterogeneous Laboratory Scale Porous Media. *Transp. Porous Media* **2004**, *54*, 107–124. [CrossRef]

47. Zhang, X.; Wu, Y. Laboratory experiments and simulations of MTBE transport in layered heterogeneous porous media. *Environ. Earth Sci.* **2016**, *75*, 836. [CrossRef]
48. Gelhar, L.W.; Welty, C.; Rehfeldt, K.R. A critical review of data on field-scale dispersion in aquifers. *Water Resour. Res.* **1992**, *28*, 1955–1974. [CrossRef]
49. Khan, A.U.H.; Jury, W.A. A laboratory study of the dispersion scale effect in column outflow experiments. *J. Contam. Hydrol.* **1990**, *5*, 119–131. [CrossRef]
50. Guiguer, N.; Horvath, M. Enviro-Base, Waterloo hydrogeologic Inc. 2003, pp. 1–7. Available online: www.waterloohydrogeologic.com (accessed on 18 September 2024).
51. Rinkel, P. Methodological Studies on Modeling Land Subsidence with the Help of Feflow Using the Example of the Ca Mau Peninsula in the Mekong Delta (Vietnam). Master's Thesis, Leibnitz University Hannover, Hannover, Germany, 2022.
52. Thanh, T.N.; Huy, T.D.; Van Kenh, N.; Tung, T.T.; Quyen, P.B.; Van Hoang, N. Methodology of determining effective porosity and longitudinal dispersivity of aquifer and the application to field tracer injection test in Southern Hanoi, Vietnam. *Vietnam J. Earth Sci.* **2017**, *39*, 57–75. [CrossRef]
53. DWRPIS. Report “Results of Experimental Water Pumping Combined Combined with Injecting Salt to BL2B.”; Internal report (in Vietnamese). Department of Water Resources Planning and Investigation South (DWRPIS): Ho Chi Minh City, Vietnam, 2021.
54. DWRPIS. Report “Results of Experimental Water Pumping Combined Combined with Injecting Salt to BL4D.”; Internal report (in Vietnamese). Department of Water Resources Planning and Investigation South (DWRPIS): Ho Chi Minh City, Vietnam, 2021.
55. DWRPIS. Report “Results of Experimental Water Pumping Combined Combined with Injecting Salt to BL5C.”; Internal report (in Vietnamese). Department of Water Resources Planning and Investigation South (DWRPIS): Ho Chi Minh City, Vietnam, 2021.
56. DWRPIS. Report “Results of Experimental Water Pumping Combined Combined with Injecting Salt to CM2E.”; Internal report (in Vietnamese). Department of Water Resources Planning and Investigation South (DWRPIS): Ho Chi Minh City, Vietnam, 2021.
57. Pechstein, A.; Hanh, H.T.; Orilski, J.; Nam, L.H.; Van Manh, L.; Chi, H.; City, M. Detailed Investigations on the Hydrogeological Situation in Ca Mau Province, Mekong Delta, Vietnam; Technical Report No III-5 of Technical Cooperation Project “Improving groundwater protection in the Mekong Delta” (Issue December); National Center for Water Resources Planning and Investigation (NAWAPI): Hanoi, Vietnam, 2018.
58. Fitts, C.R. Groundwater Science. In *Groundwater Science*; Academic Press: Cambridge, MA, USA, 2012. [CrossRef]
59. Johnson, A.I. Compilation of Specific Yields for Various Materials—Hydrologic Properties of earth Materials. Geological Survey Water-Supply Paper 1662-D 1967; 80p. Available online: <https://pubs.usgs.gov/wsp/1662d/report.pdf> (accessed on 20 October 2024).
60. Fetter, C.W. *Applied Hydrogeology*, 4th ed.; Waveland Press Inc.: Long Grove, IL, USA, 2014.
61. Freeze, R.A.; Cherry, J.A. *Groundwater*; Prentice-Hall, Inc.: Hoboken, NJ, USA, 1979.
62. Davis, P.A.; Goodrich, M.T. A proposed strategy for the validation of ground-water flow and solute transport models. In Proceedings of the GEOVAL-90, Symposium on Validation of Geosphere Performance Assessment Models, Stockholm, Sweden, 14–17 May 1990; pp. 580–588.
63. Jackson, C.P.; Lever, D.A.; Sumner, P.J. Validation of transport models for use in repository performance assessments: A view illustrated for INTRAVAL test case 1b. *Adv. Water Resour.* **1992**, *15*, 33–45. [CrossRef]
64. Rahman, A.K.M.M.; Ahmed, K.M.; Butler, A.P.; Hoque, M.A. Influence of surface geology and micro-scale land use on the shallow subsurface salinity in deltaic coastal areas: A case from southwest Bangladesh. *Environ. Earth Sci.* **2018**, *77*, 423. [CrossRef]
65. Geng, X.; Michael, H.A. Preferential Flow Enhances Pumping-Induced Saltwater Intrusion in Volcanic Aquifers. *Water Resour. Res.* **2020**, *56*, e2019WR026390. [CrossRef]
66. NAWAPI. *Forecast of the Risk of Lowering Underground Water Level and Saline Intrusion in the Mekong River Basin, Period 2021–2026*; National Center for Water Resources Planning and Investigation (NAWAPI): Hanoi, Vietnam, 2021.

Disclaimer/Publisher's Note: The statements, opinions and data contained in all publications are solely those of the individual author(s) and contributor(s) and not of MDPI and/or the editor(s). MDPI and/or the editor(s) disclaim responsibility for any injury to people or property resulting from any ideas, methods, instructions or products referred to in the content.